ANALYSIS OF NON-UNIQUE SOLUTIONS IN MEAN FIELD GAMES

BY

MICHAEL RICHARD LIVESAY

THESIS

Submitted in partial fulfillment of the requirements
for the degree of Master of Science in Electrical and Computer Engineering
in the Graduate College of the
University of Illinois at Urbana-Champaign, 2018

Urbana, Illinois

Adviser:

Professor Bruce Hajek

ABSTRACT

This thesis investigates cases when solutions to a mean field game (MFG) are non-unique. The symmetric Markov perfect information N-player game is considered and restricted to finite states and continuous time. The players' transitions are random with a parameter determined by their control. There is a unique joint distribution of the players for the symmetric Markov perfect equilibrium, but there can be multiple solutions to the MFG equations. This thesis focuses on understanding the behaviors of the many MFG solutions for the 2-state case. This thesis explores methods to determine which MFG solution represents the *fluid limit trajectories* of the N-player system for large populations.

This thesis investigates the *MFG map* which acts on the MFG distributions and outputs a prediction of the population's distribution based on the expected response of any given player. The MFG solutions are exactly the fixed points of the MFG map. The MFG solution that approximates large population trajectories is conjectured to be the only stable point for the MFG map. There is a second concept investigated, *social cost*, which is the average accumulated cost per player. But as is shown, the social cost is not a good indicator of which MFG solution approximates large population trajectories.

A set, called the *bifurcation set*, is defined by there being some possibility of multiple trajectories of a large population. Another important set is the *indifference set*, which indicates when the transition rate of the players to a state is positively reinforced by an increase of the empirical distribution of that state. However, numerical results are given, indicating that the fluid limit trajectory may relate to stability of the MFG map. It appears the MFG map is difficult to handle in many ways; stability of the mapping is difficult to show, even in a simple example and there are numerical anomalies such that non-fixed points appear to be numerically stable under rigorous tests.

To my wife and daughter, for their love and support.

ACKNOWLEDGMENTS

First and foremost I am thankful to my advisor Professor Bruce Hajek of the Electrical and Computer Engineering Department of UIUC. He introduced me to game theory and mean field games, and mentored me through a problem which he was interested in and which he determined I would strive at. Throughout the project, Bruce lead me toward problems which I could excel at solving, and prevented me from getting bogged down; in such a way as to essentially maximize my contribution in this area, for the time given.

When I requested to transfer into the ECE Department at UIUC, Bruce vouched for me, resulting in my acceptance. Hence, I hold an especial gratitude for Bruce Hajek; without him I very likely would not have had the opportunity to pursue my dream of getting a degree in engineering.

Bruce Hajek is a person of great intelligence and I deem even greater character. I am honored to have gotten to know him.

I would also like to acknowledge Peter Caines and Prashant Mehta, for a brief but enlightening encounter about the subject of mean field games. Finally, I would like to thank my doctoral advisor in Mathematics at UIUC, Professor Lee DeVille, who has brought me up in my academic maturity, and allowed me to transfer to ECE for the year.

TABLE OF CONTENTS

ABBREVIATIONS AND TERMS

- Let $\Delta_i : \mathbb{R}^d \to \mathbb{R}^d$ be the difference operator on $i \in \mathbb{N}$, given by $\Delta_i z = \begin{pmatrix} z_1 - z_i \\ z_2 - z_i \\ \vdots \\ z^d - z^i \end{pmatrix}$
- $\mathbb{N}_0 = \mathbb{N} \cup \{0\}$
- $\mathbb{R}^+ = \{x \in \mathbb{R} : x > 0\}$
- $\mathbb{R}_0^+ = \{x \in \mathbb{R} : x \geq 0\}$
- $t \vee s = \max\{t, s\}$
- $t \wedge s = \min\{t, s\}$
- MFG means "mean field games"
- ITVP means "initial-terminal value problem"
- IVP means "initial value problem"
- TVP means "terminal value problem"
- IC means "initial condition"
- TC means "terminal condition"
- ITC means "initial-terminal condition"
- CTCS means "continuous time continuous states"
- CTDS means "continuous time discrete states"

1 INTRODUCTION

Mean field game (MFG) theory is the study of decision-making policies for a large number of rational players, each with relatively small influence on the population's distribution over the states of a game. The MFG was discovered in 2006 by Huang, Malhame, and Caines [1], and independently by Lasry and P. L. Lions in 2007 [2]. In Huang et al. [1] and Lasry et al. [2] continuous state continuous time (CSCT) models are considered, and the analysis is based on the Hamilton-Jacobi-Bellman (HJB) and the Fokker-Planck-Kolmogorov equations. The MFG model has applications in optimal control theory, economics, engineering, and social planning [3], [4], [5], [6].

The purpose of MFGs is to approximate the trajectory of a large population's distribution over the states in the game. The symmetric Markov perfect equilibrium for the N-player game requires that each player considers the options of the other players, the number of considerations is combinatorially explosive. This can be rectified for large populations by instead working with the mean field game system, which does not depend on the number of players. There has been much work examining under what conditions the limit trajectories converge to a unique solution of the MFG system, see [1], [2], [7], [8], [9], [10] and especially [3]. In this thesis, the primary interest is for non-unique solutions to the MFG, in particular contrasting the different solutions to determine the approximate trajectory of a large population. In the work of Yin, Mehta, Meyn, and Shanbhag [11] in 2012, an MFG (oscillator) model is shown to have non-unique solutions.

Chapter 2 adopts the discrete state continuous time (DSCT) MFG model given by Gomes, Mohr, and Souza in 2013 [7]. This system also includes the Hamilton-Jacobi (HJ) and the Kolmogorov equations. Also, in this chapter, the objective of this research is given, which (in short) is to analyze methods of parsing through multiple solutions of the MFG system

to find which one models large populations. This thesis restricts attention to the 2-state case with costs of a particular form. In Chapter 3, one tractable example of *follow the crowd* type cost which has multiple solutions is thoroughly analyzed, and traits of the different solutions are observed. Early on in this chapter, another tractable example of *avoid the crowd* type cost is shown to have a unique solution despite that it fails the sufficient conditions laid out in Gomes et al. [7] for uniqueness. In Chapter 4, methods are tested against different examples, illustrating the difficulties in numerically searching for the limit trajectory when multiple solutions of the MFG exist. Early on in this chapter, stability of the MFG solution is discussed for a particular case.

2 MEAN FIELD GAME OVERVIEW

The discrete state continuous time (DSCT) mean field game model, as given in Gomes et al. [7], is adopted. This system includes Hamilton-Jacobi (HJ) equations and the Kolmogorov equation. Theorem 2.1.1 in Gomes et al. [7] gives a method to solve for the common equilibrium policies. The reduced 2-state model is given and refined, see (2.18), and is used throughout this document. The objective of this research is to discover a method for finding which of the multiple solutions of the MFG system models large populations. In the final section of this chapter, Section 2.3, a proposed method for finding the population's trajectory is based on *stability of the MFG map*, and this is explored more carefully in Chapter 4. A second viable method is described as the lowest social cost of the MFG solutions, but is shown to fail.

2.1 Model

Consider a symmetric Markov N-player game with perfect information, where each player is in a state from a finite set of states $I^d = \{1, ..., d\}$ in continuous time and players adjust their control in order to minimize their cost. The paper Gomes et al. [7], considers such games, and analyzes the corresponding MFG. The setting of the MFG in Gomes et al. [7] is paraphrased in this section.

Given a reference player, the set of probability distributions of other players among the states is given by $\mathcal{S}^d$. The control for a reference player is given by $\alpha \in (\mathbb{R}_0^+)^{d\times d}$, it describes the rate at which the player tries to move from one state to any other state. The control function is $\alpha : [0, T] \to (\mathbb{R}_0^+)^{d\times d}$. For convenience, define $\alpha_j(i, t) := \alpha_{ij}(t)$; this is the control for the reference player to go from state i to state j.

Consider the running cost $c : I^d \times \mathcal{S}^d \times (\mathbb{R}_0^+)^d \to \mathbb{R}$ given in Gomes et al. [7]. It is assumed that $c(i, \theta, \alpha)$ does not depend on α_i, else a player may accumulate cost for trying to stay in their current state. Both c and $\frac{\partial c}{\partial \alpha}$ are assumed to be Lipschitz continuous with respect to θ. It is assumed that $c(i, \theta, \alpha)$ is strongly convex in α, that is, for some $\gamma > 0$

$$c(i, \theta, \alpha') - c(i, \theta, \alpha) \geq \nabla_\alpha c(i, \theta, \alpha) \cdot (\alpha' - \alpha) + \gamma \|\alpha' - \alpha\|^2.$$

The running cost is superlinear in α_j, that is $\lim_{\alpha_j \to \infty} \frac{c(i,\theta,\alpha)}{\|\alpha\|} \to \infty$ for $j \neq i$. There is a terminal cost denoted as $\psi_i(\theta(T))$ which is Lipschitz continuous with respect to $\theta(T)$.

Before seeing how the N player game transpires, the game is reduced to a single reference player assuming that all other players' trajectories are known. To a great extent this simplifies the problem. The solution for the reference player is dependent only on the variable distribution of all players over time. Suppose the empirical distribution of the other players (not including the reference player) as a function of time is given by $\theta : [0, T] \to \mathcal{S}^d$ to the reference player. Thus the reference player's control response depends on future values of θ and hence the system is non-causal. Finally assume i is the state of the reference player at time t. The cost-to-go for the reference player using a control policy $\alpha = (\alpha(t) : 0 \leq t \leq T)$ is given by

$$u_i^\theta(t, \alpha) = \mathbb{E}^\alpha \left[\int_t^T c(\mathbf{i}_s, \theta(s), \alpha(s)) ds + \psi_{\mathbf{i}_T}(\theta(T)) \middle| \mathbf{i}_t = i \right], \tag{2.1}$$

and transition rate of the reference player's state is determined by the control α according to the continuous time discrete state (CTDS) Markov process

$$\mathbb{P}[\mathbf{i}_{t+h} = j | \mathbf{i}_t = i] = \alpha_{ij}(t)h + o(h). \tag{2.2}$$

The value function or the minimal cost-to-go is

$$u_i^\theta(t) = \min_\alpha \left\{ u_i^\theta(t, \alpha) \right\}. \tag{2.3}$$

The control associated to the minimal cost-to-go is the rational player's choice. Consider the Legendre transform of the running cost

$$h(i,\theta,\Delta_i z) = \min_{\alpha\in(\mathbb{R}_0^+)^d}\{c(i,\theta,\alpha)+\alpha\cdot\Delta_i z\}. \tag{2.4}$$

By convexity and superlinearity of the running cost, $\operatorname{argmin}_{\alpha\in(\mathbb{R}_0^+)^d}\{c(i,\theta,\alpha)+\alpha\cdot\Delta_i z\}$ is well defined at each coordinate except the i^{th} coordinate, where there is no constraint at all because $c(i,\theta,\alpha)+\alpha\cdot\Delta_i z$ is independent of the α_i coordinate. Hence the following is well defined

$$\begin{cases} \alpha^*(i,\theta,\Delta_i z) & \in \operatorname{argmin}_{\alpha\in(\mathbb{R}_0^+)^d}\{c(i,\theta,\alpha)+\alpha\cdot\Delta_i z\} \\ \alpha^*_{i,i}(\theta,\Delta_i z) & = -\sum_{j\neq i}\alpha^*_{i,j}(\theta,z). \end{cases} \tag{2.5}$$

Given a single reference player and the distribution of the other players, θ, for all time, consider the Hamilton-Jacobi (HJ) ordinary differential equations (ODE) with terminal condition (TC) for the game

$$\begin{cases} -\dfrac{d}{dt}u_i = h(i,\theta,\Delta_i u) \\ u_i(T) = \psi_i(\theta(T)). \end{cases} \tag{2.6}$$

Suppose the distribution of the other players is not given, although at any given time of the game all players can observe each of the N players' current state. Suppose that the non-reference players choose some strategy, and the reference player has the same objective as before, to minimize cost. Suppose that each player's cost function is dependent on the distribution of the other players and the player's state. Since all players know that they are playing against a rational population they will take into consideration the other players' strategies, causing the problem to be intractable. The relationships between the $N+1$ rational players are complex, because each player has to account for the other players' expected behavior, but this prediction is recursive as the players know that the others

are making such an account. To model these $N+1$ rational players a more complicated system than (2.6) is required.

Suppose that there are $N+1$ players. The reference player knows the other players' strategy β. Suppose that $\mathbf{i}$ is the reference player's state and $\mathbf{n}$ is the number of the other N players in each state, that is $\frac{\mathbf{n}}{N} \in \mathcal{S}_N^d = \{\frac{\mathbf{n}}{N} \in \mathbb{Z}^d : \sum_{i \in I^d} \mathbf{n}_i = N\}$ is the distribution of the other N players. The reference player wants to minimize cost-to-go, given by

$$u_i^n(t,\alpha,\beta) = \mathbb{E}^{\alpha,\beta}\left[\int_t^T c\left(\mathbf{i}_s, \frac{\mathbf{n}_s}{N}, \alpha\left(s, \mathbf{i}_s, \frac{\mathbf{n}_s}{N}\right)\right) ds + \psi_{\mathbf{i}_T}\left(\frac{\mathbf{n}_T}{N}\right) \middle| \mathbf{i}_t = i, \mathbf{n}_t = n\right], \tag{2.7}$$

where α is the reference player's strategy.

Suppose that $e_{ij} = e_i - e_j$ and e_i is the i-th vector of the canonical basis of $\mathbb{R}^d$. Let $\mathbf{n}$ be so that $\frac{\mathbf{n}}{N} \in \mathcal{S}_N^d$ where $\mathbf{n}_i$ is the number of players in state i, not including the reference player. The following determines the cost-to-go functions for the $N+1$ rational players, as given in Gomes et al. [7]

$$\begin{cases} -\dfrac{d}{dt}u_i^n = h\left(i, \dfrac{n}{N}, \Delta_i u^n\right) + \displaystyle\sum_{k,j} n_k \beta_{kj}\left(\frac{n+e_{ik}}{N}, u_i^{n+e_{ik}}\right)\left(u_i^{n+e_{jk}} - u_i^n\right) \\ u_i^n(T) = \psi_i\left(\dfrac{n}{N}\right). \end{cases} \tag{2.8}$$

The transition rate of the reference player's state for the $N+1$ player game is determined by the control α according to the continuous time discrete state (CTDS) Markov process

$$\mathbb{P}[\mathbf{i}_{t+h} = j | \mathbf{n}_t = n, \mathbf{i}_t = i] = \alpha_{ij}\left(\frac{n}{N}, u^n\right) h + o(h), \tag{2.9}$$

and the transition rates of the other N players are given by

$$\mathbb{P}[\mathbf{n}_{t+h} = n + e_{jk} | \mathbf{n}_t = n, \mathbf{i}_t = i] = n_k \beta_{kj}\left(\frac{n+e_{ik}}{N}, u^{n+e_{ik}}\right) h + o(h). \tag{2.10}$$

The control profile $(\alpha, \alpha, ..., \alpha)$ is a Nash equilibrium if α minimizes the quantity on the

right-hand side of (2.7) for $\beta = \alpha$. In Gomes et al. [7] it is shown that a Markov perfect equilibrium exists, and $(\alpha^*, \alpha^*, ..., \alpha^*)$ is a Markov perfect equilibrium.

For large populations, given a marginal distribution of their actions and a small time interval, the fraction of players who move from one state to another is approximated by its expectation–by the law of large numbers. The motivation for MFG is, for large enough populations, to predict the force of the masses on the individual. It is impossible to know what any individual is doing, but the control for each individual is deterministic, given the flow of the masses. The MFG model is such that each player has a cost-to-go given by the HJ (or Hamilton-Jacobi-Bellman) equation which depends on the populations' trajectory given in (2.6), while the entire populations' trajectory adheres to the Fokker-Planck-Kolmogorov equation determined by their cost-to-go. The MFG model given in Gomes et al. [7] is

$$\begin{cases} -\dfrac{d}{dt}u_i = h(i, \theta, \Delta_i u), & u_i(T) = \psi_i(\theta(T)) \\ \dfrac{d}{dt}\theta_i = \displaystyle\sum_j \theta_j \alpha^*_{j,i}(\theta, \Delta_j u), & \theta(0) = \bar{\theta} \in [0,1]^d, \text{ with } \displaystyle\sum_{i=1}^{N} \bar{\theta}_i = 1. \end{cases} \tag{2.11}$$

2.1.1 2-State Model

In this section (2.6), (2.8), and (2.11) are specialized to the 2-state case. The case of 2-states allows for a one-dimensional representation of the population's distribution. In general, the 2-state case is equipped with the state space $\{0, 1\}$ instead of $\{1, 2\}$ (for convenience). For $\theta \in [0, 1]^2$ and $\theta_1 = 1 - \theta_0$, the vector θ is determined by either of its coordinates. Thus in the 2-state case the distribution can be denoted by $\begin{pmatrix} \theta \\ 1-\theta \end{pmatrix}$, where θ is the fraction of players in state 0.

The running cost for a given player depends on the state, i, that the player is in, the fraction, θ, of players in state 0, and the control, $\alpha_{i,1-i}$, from state i to state $1 - i$. Assume throughout this section that the form of the running cost is $c(i, \theta, \alpha) = f(i, \theta) + \alpha^2_{i,1-i}/2$.

Equation (2.5) reduces to

$$\begin{cases} \alpha^*_{i,1-i}(\theta, z) = \underset{\alpha \in (\mathbb{R}_0^+)^2}{\operatorname{argmin}} \{c(i, \theta, \alpha) + \alpha \cdot \Delta_i z\} \\ \\ \alpha^*_{i,i}(\theta, z) = -\alpha^*_{i,1-i}(\theta, z). \end{cases} \tag{2.12}$$

In Gomes et al. [7] a "verification theorem" was given for both cases of one reference player against deterministic population and for $N + 1$ rational players. The proof uses Dynkin's formula. The result for one player given a deterministic population states that given a solution u to (2.6), the $\alpha^*(\cdot, u)$ which minimizes the Legendre transform of the running cost is also the strategy used to minimize the cost-to-go.

Theorem 2.1.1 gives the optimal control α^* for the 2-state case where the running cost has the form $c(i, \theta, \alpha) = f(i, \theta) + \alpha^2_{i,1-i}/2$. This particular form of the running cost is used throughout Chapters 3 and 4.

Theorem 2.1.1. *Suppose that the running cost is of the form $c(i, \theta, \alpha) = f(i, \theta) + \alpha^2_{i,1-i}/2$, for some fixed $\theta := \theta_{[0,T]}$. Then $\alpha^*(\theta, u)$ minimizes u_i^θ defined in* (2.1)*. Moreover α^* defined in* (2.5) *is given by $\alpha^*_{i,1-i}(\theta, z) = (z_i - z_{1-i})_+$.*

Proof. See Gomes et al. [7] for proof that $\alpha^*(\theta, u)$ minimizes the right-hand side of (2.1).

By definition

$$\begin{aligned} \alpha^*_{i,1-i}(\theta, z) &= \underset{\alpha \geq 0}{\operatorname{argmin}} \{c(i, \theta, \alpha) + \alpha_{i,1-i}(z_{1-i} - z_i)\} \\ &= \underset{\alpha \geq 0}{\operatorname{argmin}} f(i, \theta) + \frac{\alpha^2_{i,1-i}}{2} + \alpha_{i,1-i}(z_{1-i} - z_i) \\ &= \underset{\alpha \geq 0}{\operatorname{argmin}} \left(\frac{1}{2}\alpha^2_{i,1-i} + (z_{1-i} - z_i)\alpha_{i,1-i} \right) \\ &= (z_i - z_{1-i})_+. \end{aligned} \tag{2.13}$$

□

When using the tractable form of running cost $c(i, \theta, \alpha) = f(i, \theta) + \alpha^2_{i,1-i}/2$; both (2.6)

and (2.8) simplify. Given a distribution $\theta(t)$ for $t \in [0,T]$, (2.6) becomes

$$\begin{cases} -\dfrac{d}{dt}u_i = f(i,\theta) - \dfrac{1}{2}(u_i - u_{1-i})_+^2 \\ u_i(T) = \psi_i(\theta(T)), \end{cases} \tag{2.14}$$

and hence the Markov transition probabilities are

$$\mathbb{P}[\mathbf{i}_{t+h} = 1-i | \mathbf{i}_t = i] = (u_i(t) - u_{1-i}(t))_+ h + o(h). \tag{2.15}$$

System (2.8) is now

$$\begin{cases} -\dfrac{d}{dt}u_i^n = f\left(i, \dfrac{n}{N}\right) - \dfrac{1}{2}(u_i^n - u_{1-i}^n)_+^2 + \\ \qquad + n\alpha_{0,1}^*\left(\dfrac{n-i}{N}, u^n\right)[u_i^{n+1} - u_i^n] + (N-n)\alpha_{1,0}^*\left(\dfrac{n+1-i}{N}, u^n\right)[u_i^{n-1} - u_i^n] \\ u_i^n(T) = \psi_i\left(\dfrac{n}{N}\right), \end{cases} \tag{2.16}$$

hence the transition rates are

$$\begin{aligned} &\mathbb{P}[\mathbf{i}_{t+h} = 1-i | \mathbf{n}_t = n, \mathbf{i}_t = i] = \alpha_{i,1-i}^*\left(\frac{n}{N}, u^n\right) h + o(h), \\ &\mathbb{P}[\mathbf{n}_{t+h} = n-1 | \mathbf{n}_t = n, \mathbf{i}_t = i] = n\alpha_{0,1}^*\left(\frac{n-i}{N}, u^{n-i}\right) h + o(h) \text{ and} \\ &\mathbb{P}[\mathbf{n}_{t+h} = n+1 | \mathbf{n}_t = n, \mathbf{i}_t = i] = (N-n)\alpha_{1,0}^*\left(\frac{n+1-i}{N}, u^{n+1-i}\right) h + o(h). \end{aligned} \tag{2.17}$$

The MFG model given by (2.11) becomes

$$\begin{cases} -\dot{u}_0 = f(0,\theta) - \dfrac{1}{2}(u_0 - u_1)_+^2 \\ -\dot{u}_1 = f(1,\theta) - \dfrac{1}{2}(u_1 - u_0)_+^2 \\ \dot{\theta} = -\theta(u_0 - u_1)_+ + (1-\theta)(u_1 - u_0)_+ \\ u_i(T) = \psi_i(\theta(T)), \theta(0) = \bar{\theta} \in [0,1]. \end{cases} \tag{2.18}$$

2.2 Objective of Study

In this section the objective of the study is outlined. A definition of *fluid limit trajectory* is presented. The fluid limit trajectories are the trajectories this thesis considers most meaningful. The *bifurcation set*, is a set where the number of fluid limit trajectories coming from a single initial distribution is not one.

Definition 2.2.1. *Consider the symmetric Markov perfect equilibrium for the $N+1$ rational player game given by* (2.8)-(2.10)*, with all players using the strategy α^* minimizing the average cost in* (2.7)*. Suppose that $\mathbf{n}^N$ is the distribution of the N non-reference players with transition rates* (2.10)*. Suppose that $\theta : [0,T] \to \mathcal{S}_N^d$.*

Then θ is a fluid limit trajectory *if for some $\{x^N\}_{N=1}^{\infty}$ with $\lim_{N\to\infty} \frac{x^N}{N} \to \theta(0)$, the following holds for any $\epsilon > 0$,*

$$\lim_{N\to\infty} \mathbb{P}\left[\left\| \frac{\mathbf{n}^N}{N} - \theta \right\|_{\infty} < \epsilon \,\middle|\, \mathbf{n}^N(0) = x^N \right] = 1. \tag{2.19}$$

Consider the MFG model given by (2.11). Since this system is an ITVP, even Lipschitz conditions are not enough to guarantee unique solutions. Indeed, solutions to mean field games are not necessarily unique. Figure 2.1 gives an example of non-unique solutions for the 2-state MFG given by (2.18). This example is thoroughly analyzed in Chapter 3. When presented with multiple solutions there are two immediate questions.

1. Does one of the solutions to the MFG model given by (2.11) represent the fluid limit trajectory determined by the transition rates given by (2.10)?

2. If so, how can it be determined which solutions of the MFG model given by (2.11) represent the fluid limit trajectories given by (2.10), without directly computing the fluid limit trajectory?

Both are open problems. In view of these questions, there is a relevant set of points that dictate which MFG solutions are fluid limit trajectories over all times to play. If this set

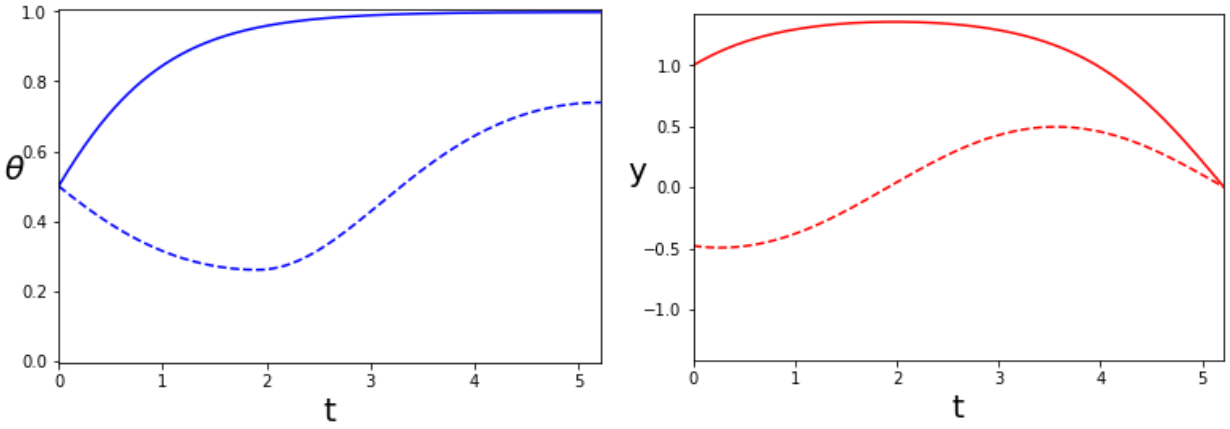

Figure 2.1: Consider (2.18) with $f(i,\theta) = |\theta - (1-i)|$ in the running cost, with initial terminal conditions (ITC) $\theta(0) = 1/2$ and $\psi_i \equiv 0$, and the time to play $T = 3$. On the left are two solutions of θ, the fraction in state 0. On the right are the corresponding cost-to-go differences $y := u_1 - u_0$. The solid lines in both graphs represent the fluid limit trajectory which is also an MFG solution. Note that not all solutions of the MFG system are plotted.

was known, then any MFG solution can be determined to be a fluid limit trajectory based on whether it crosses the set.

Definition 2.2.2. *Consider the symmetric Markov perfect equilibrium for the $N+1$ rational player game given by* (2.8). *The* bifurcation set *is the set of points (T, μ) so that $T > 0$ is the time to play and there is not exactly one fluid limit trajectories with initial distribution μ.*

Conjecture 2.2.3. *For any initial distribution there is at least one fluid limit trajectory, and all fluid limit trajectories solve the MFG model given by* (2.11). *The fluid limit trajectories do not cross the bifurcation set.*

In Cardaliaguet et al. [3] it is proven that under certain conditions, for the continuous state case, the trajectories of the N rational players to the solution of the MFG converge in expectation. Unfortunately, uniqueness of the solution was one of the conditions assumed.

2.3 Methods for Fluid Limit Trajectories and MFG Solutions

In this section two analytic methods are discussed for the purpose of determining whether a MFG solution for a given time to play is a fluid limit trajectory. The first is determining the stable points of a particular mapping of population trajectories, the MFG map. The question is whether the fluid limit trajectories are exactly the stable fixed points of the MFG map. This is examined in more depth in Chapter 4, but an introduction to it is given in Section 2.3.1. The second method is determining the MFG solution with the minimum *social cost* which is covered in Section 2.3.2 where a conjectured method to find the fluid limit trajectory is given and shown to fail.

2.3.1 Stability of the MFG Map

Suppose a politician were to give the future distribution, θ. Suppose that each player believed this politician. Then all players will develop the same policy which optimizes their performance based on this assumed behavior. Each player's policy is determined by (2.6), and their trajectory flows according to (2.2). The MFG map is derived by using the Kolmogorov equation to determine the resulting flow of the population's distribution. The MFG map is discussed in Gomes et al. [7], with notation ξ, to show existence of MFG solutions. The purpose was not to look at properties of stability nor to distinguish between multiple MFG solutions for the fluid limit trajectory. The following is the definition of the MFG map.

Definition 2.3.1. *Consider the MFG model given by* (2.11) *given a time to play T and running cost c. Suppose that a predicted fractional population trajectory $\theta := (\theta(t) : 0 \leq t \leq T)$ is given. Define the MFG map, denoted Φ, on θ as the solution to*

$$\begin{cases} \dfrac{d}{dt}\tilde{\theta}_i = \displaystyle\sum_j \tilde{\theta}_j \alpha^*_{j,i}(\tilde{\theta}, \Delta_j u), \\ \tilde{\theta}(0) = \theta(0), \end{cases} \tag{2.20}$$

where the vector function $u := (u_{c,T,\theta}(t) : 0 \le t \le T)$ *is the solution to*

$$\begin{cases} -\dfrac{d}{dt}u_i = h(i, \theta, \Delta_i u) \\ u_i(T) = \psi_i(\theta(T)). \end{cases} \tag{2.21}$$

That is $\Phi(\theta) = \tilde{\theta}$.

The functions (θ, u) solve the MFG if and only if $\Phi(\theta) = \theta$. In other words, the MFG solutions are exactly the fixed points of the MFG map. The following conjecture is investigated in Chapter 4.

Conjecture 2.3.2. *The stable fixed points of the MFG map* Φ *are exactly the fluid limit trajectories.*

Given a prediction θ there is no guarantee that $\lim_{n\to\infty} \Phi^n(\theta)$ exists (Φ^n is the n-fold composition of Φ). In fact, there are examples where $\Phi^n(\theta)$ oscillates between two functions, and a prediction θ can be above the bifurcation set while the map $\Phi(\theta)$ is below the set. One such example, shown in Fig. 2.2, is for the MFG model given by (2.18) where

$$f(i, \theta) = |1 - i - \theta| + 8(\theta - 0.75)\mathbb{1}_{\{\theta > 0.75\}} + 8(0.25 - \theta)\mathbb{1}_{\{\theta < 0.25\}}.$$

Recall the MFG map Φ. Define $\Phi_M : \theta \mapsto \frac{M-1}{M}\theta + \frac{1}{M}\Phi(\theta)$, for any $M \in \mathbb{N}$, and define $\Psi_M \equiv \Phi_M^M$. Suppose instead of applying Φ^n to the initial prediction θ, the map Ψ_M^n is applied for some $M \in \mathbb{N}$, (Ψ^n is the n-fold compositions of Ψ). Because the steps are smaller, the operation Ψ_M takes longer to compute than Φ, but it will not jump as far and so is more likely to converge.

Recall the running cost function $c(i, \theta, \alpha) = |1 - i - \theta| + 8(\theta - 0.75)\mathbb{1}_{\{\theta > 0.75\}} + 8(0.25 - \theta)\mathbb{1}_{\{\theta < 0.25\}} + \alpha_{i,1-i}^2/2$ from Section 2.3.1, and Fig. 2.2. The map Ψ_M is used instead of Φ to illustrate stability of the MFG map Φ, see Fig. 2.3. It is conceivable that under sufficient conditions $\Psi := \lim_{M\to\infty} \Psi_M$ exists, and has a form where stability of Ψ is more simple to show than that of Φ. But no further analysis of Ψ_M is given here.

Examples exist (see Chapter 4 for details) with MFG solutions that are not fluid limit

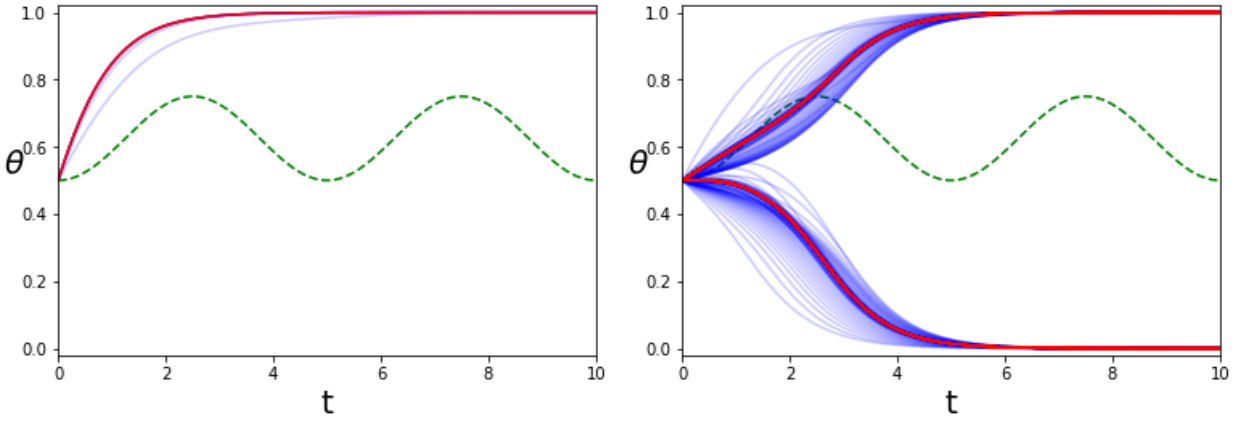

Figure 2.2: Each plot contains multiple iterations of the MFG map applied to Φ to the same initial distribution. In both plots the MFG has no terminal cost. To the left the running cost is $c(i, \theta, \alpha) = |1 - i - \theta| + \alpha_{i,1-i}^2/2$. To the right the running cost is $c(i, \theta, \alpha) = |1 - i - \theta| + 8(\theta - 0.75)\mathbb{1}_{\{\theta>0.75\}} + 8(0.25 - \theta)\mathbb{1}_{\{\theta<0.25\}} + \alpha_{i,1-i}^2/2$. There is non-negative initial prediction $\theta(t) = 0.5 + 0.25\sin^2(2\pi t)$ given, plotted, in green. Then the first 200 iterations of Φ are applied to the initial prediction and plotted, in blue. In red, on the left is the limit of the converging sequence of functions; and also in red, on the right an additional twenty iterations of Φ are plotted to illustrate that $\Phi^{2n}(\theta)$ and $\Phi^{2n+1}(\theta)$ appear to converge.

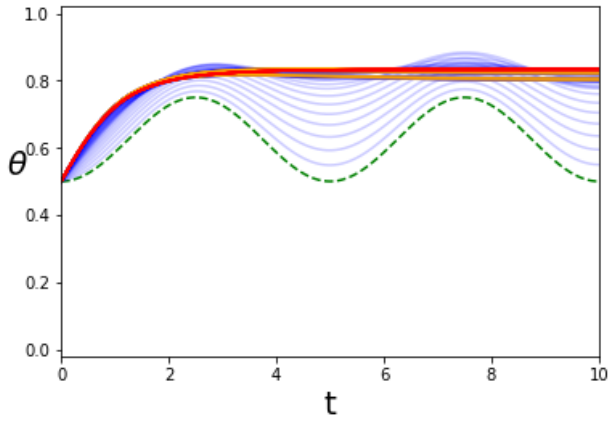

Figure 2.3: Illustration of improved convergence properties of Ψ vs Φ. The costs and initial prediction are the same as in as in the second plot of Fig. 2.2. In blue are $\Psi_{10}^n(\theta)$ for $n \in \{1, 2, ..., 100\}$. In orange are $\Psi_{10}^n(\theta)$ for $n \in \{101, 102, ..., 200\}$, which are oscillating. In red are $\Psi_{100}^n \Psi_{10}^{200}(\theta)$ for $n \in \{1, 2, ..., 100\}$.

trajectories but appear numerically stable. This behavior may be attributed to a numerical phenomenon. Even worse examples exist attributed to this numerical phenomenon where a non-fixed point of the MFG map is numerically stable, this appears to be very common. Thus, finding MFG solutions that are not fluid limit trajectories, but which appear to be numerically stable, does not refute Conjecture 2.3.2 because the solutions could be pseudo stable only. Due to examples like these, even if Conjecture 2.3.2 were proven to be true, it is not immediately obvious how to find the fluid limit trajectories. This is all discussed in Chapter 4, and moreover the Gâteaux derivative of Φ is exploited to analyze stability of the mapping at an MFG solution in Chapter 4.

2.3.2 Social Cost of MFG Solution

The social cost of a MFG solution is the total cost per player averaged over all players. It is well known that in a perfect information game there may be a Nash equilibrium which is not optimal for the social cost, such as with the prisoners' dilemma. One could ask the less obvious question of whether or not a fluid limit trajectory has the lowest social cost amongst all MFG solutions. It will be illustrated that the fluid limit trajectory does not necessarily have smaller social cost than the MFG solutions.

Definition 2.3.3. *Given a solution (θ, u) for the MFG model given by* (2.11)*, the social cost is given by $\sum_i \theta_i(0)u_i(0)$.*

Of course Nash equilibriums do not have to minimize social cost, and so one should expect that there are population trajectories which have strictly smaller social cost than all MFG solutions. But of the MFG solutions, all players are minimizing their expected costs based on their knowledge of the other rational players. Hence it would not be too surprising if the fluid limit trajectory was the MFG solution with the lowest social cost.

Suppose the number of players, N, is given and consider (2.18). Suppose the system has time to play $T = 3$, running cost $c(i, \theta, \alpha) = |1 - i - \theta| + \alpha^2_{i,1-i}/2$, and terminal cost

$\psi_0(\theta) = 0$ and $\psi_1(\theta) = 0.3$; see Fig. 2.4. Consider the set of points

$$\mathcal{U}_N = \{(t, \theta) \in [0, T] \times [0, 1] : u_1^n(t, \theta) - u_0^n(t, \theta) > 0\}.$$

The largest value of θ for points in the complement of U_N is about 0.3458, so giving the players' a strictly larger initial distribution say, $\theta = 0.375$, guarantees that the trajectories of the players are monotonically increasing. The fluid limit trajectory with this initial distribution has the social cost of 1.10057 while one MFG solution has a lower social cost of 1.04352.

The three MFG solutions for IC $\theta(0) = \frac{69.5}{201} \approx 0.3458$ are shown in the top right plot of Fig. 2.4, with their social costs. The top left plot is an illustration of U_N where $N = 200$. The set of points U_N are in black and its complement in white. On the bottom the solid line indicates the fluid limit trajectory, the dashed lines indicate the other MFG solutions. The plot in the bottom left shows 20 trajectories with IC $\theta(0) = \frac{70}{201}$ and 20 trajectories with IC $\theta(0) = \frac{69}{201}$ for the 201 rational player game. The bottom right shows plots of the three MFG solutions overlaid with 50 trajectories given IC $\theta(0) = \frac{75}{201}$ of the 201 rational players. The plot on the bottom right is thus a counterexample to the conjecture that the MFG solution with smallest social cost is a fluid limit trajectory. The highest white point is attained when the fraction of players in state 0 is about 0.3458. Observe that the fluid limit trajectory does not have lowest social cost among the MFG solutions.

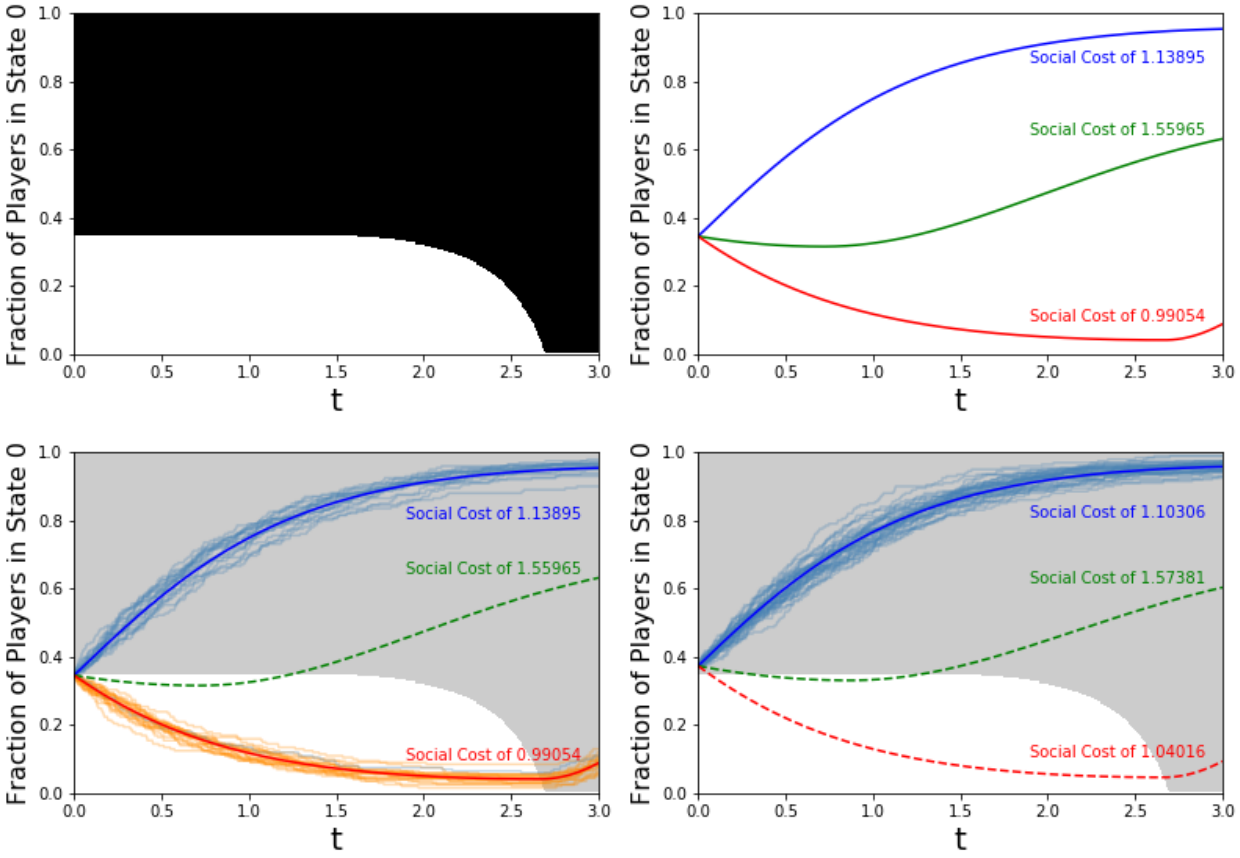

Figure 2.4: Counterexample, showing that a fluid limit trajectory is not necessarily an MFG solution with minimum social cost.

3 ANALYSIS OF AN MFG WITH NON-UNIQUE SOLUTIONS

This chapter focuses on the MFG model given by (2.18) for two tractable examples. In both cases the form of the running cost is $c(i,\theta,\alpha) = f(i,\theta)+\alpha_{i,1-i}^2/2$ and there is no terminal cost. Neither example satisfies the monotonicity conditions which guarantee uniqueness shown in Gomes et al. [7]. Section 3.1 gives a model of a population which desires to avoid the crowd. This example has a unique solution despite failing the aforementioned monotonicity condition. The avoid the crowd model acts as a contrasting model to the follow the crowd model introduced in Section 3.2 which is the primary model of this chapter. Section 3.3 is devoted to identifying the number of solutions to (3.5) and is summarized in Theorem 3.3.1.

3.1 2-State Avoid the Crowd Case

The first case study is of the *avoid the crowd* kind, where the players try to avoid highly congested areas. This will serve as a contrasting example to our later follow the crowd populations. Taking a passage from Cardaliaguet et al. [3], "The interpretation of the monotonicity condition is that the players dislike congested areas and favor configurations in which they are more scattered." However, Cardaliaguet et al. [3] worked with continuous states and their monotonicity conditions are different than in Gomes et al. [7]. Nevertheless, the previous quote may serve as an indication of what might be expected in the discrete state case.

In this section assume the running cost function is given by $c(i,\theta,\alpha) = |i-\theta| + \alpha_{i,1-i}^2/2$.

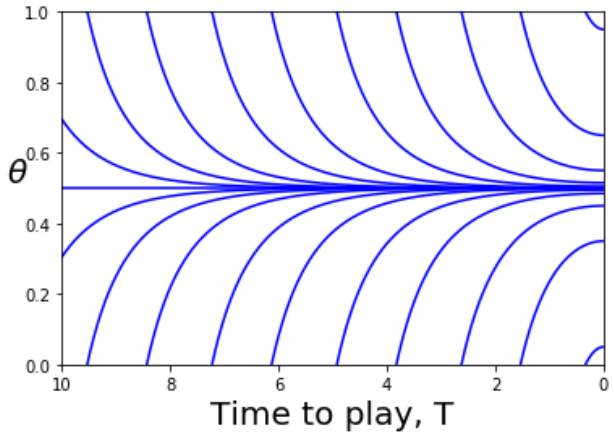

Figure 3.1: Symmetric avoid the crowd solutions. Given an initial condition (IC) and time to play T, a solution to (3.1) would simply follow the contour. Uniqueness is indicated in the picture, as the contours do not cross.

With this cost, (2.18) becomes

$$\begin{cases} -\dot{u}_0 = \theta - \frac{1}{2}(u_0 - u_1)_+^2, & u_0(T) = 0 \\ -\dot{u}_1 = 1 - \theta - \frac{1}{2}(u_1 - u_0)_+^2, & u_1(T) = 0 \\ \dot{\theta} = -\theta(u_0 - u_1)_+ + (1-\theta)(u_1 - u_0)_+, & \theta(0) = \bar{\theta}. \end{cases} \tag{3.1}$$

One of the monotonicity conditions outlined in Gomes et al. [7] is not satisfied by (3.1), despite its avoid the crowd type running cost. Still, the tractable (3.1) has a unique solution; see Fig. 3.1.

Assumption 1: The first assumption is simply

$$\sum_i (\theta_i - \tilde{\theta}_i)(\psi_i(\theta) - \psi_i(\tilde{\theta})) \geq 0.$$

This assumption is trivially satisfied by (3.1) because $\psi \equiv \mathbf{0}$.

Assumption 2: Consider the orthogonal projection, P, which projects onto the complement of the one dimensional vector space containing $\mathbf{1}$. The assumption is that for any

$M > 0$ there exists a $\gamma_i > 0$ so that if $\|Pz\| \leq M$ then

$$h(i, \theta, \Delta_i z) - h(i, \theta, \Delta_i w) - \alpha^*(i, \theta, w) \cdot (\Delta_i z - \Delta_i w) \leq -\gamma_i \|\Delta_i z - \Delta_i w\|^2.$$

For (3.2), if $(z_i - z_{1-i}), (w_i - w_{1-i}) < 0$ then

$$\begin{aligned} &h(i, \theta, \Delta_i z) - h(i, \theta, \Delta_i w) - \alpha^*(i, \theta, w) \cdot (\Delta_i z - \Delta_i w) \\ &\qquad = -\frac{(z_i - z_{1-i})_+^2}{2} + \frac{(w_i - w_{1-i})_+^2}{2} - (w_i - w_{1-i})_+((z_{1-i} - z_i) - (w_{1-i} - w_i)) \\ &\qquad = 0 \\ &\qquad > -\gamma_i((z_{1-i} - z_i) - (w_{1-i} - w_i))^2. \end{aligned}$$

Hence this condition fails.

Assumption 3: Define

$$h(\theta, z) := \begin{pmatrix} h(0, \theta, \Delta_0 z) \\ h(1, \theta, \Delta_1 z) \end{pmatrix} = \begin{pmatrix} \theta - \frac{1}{2}(z_0 - z_1)_+^2 \\ 1 - \theta - \frac{1}{2}(z_1 - z_0)_+^2 \end{pmatrix}.$$

There exists $\gamma > 0$ so that for $\theta, \tilde{\theta} \in [0, 1]$

$$\begin{pmatrix} \theta \\ 1 - \theta \end{pmatrix} \cdot (h(\tilde{\theta}, z) - h(\theta, z)) + \begin{pmatrix} \tilde{\theta} \\ 1 - \tilde{\theta} \end{pmatrix} \cdot (h(\theta, \tilde{z}) - h(\tilde{\theta}, \tilde{z})) \leq -\gamma \left\| \begin{pmatrix} \theta \\ 1 - \theta \end{pmatrix} - \begin{pmatrix} \tilde{\theta} \\ 1 - \tilde{\theta} \end{pmatrix} \right\|^2.$$

The cost passes this condition for $\gamma = 1$ because

$$\begin{aligned}\begin{pmatrix} \theta \\ 1-\theta \end{pmatrix} \cdot (h(\tilde{\theta}, z) - h(\theta, z)) + \begin{pmatrix} \tilde{\theta} \\ 1-\tilde{\theta} \end{pmatrix} \cdot (h(\theta, \tilde{z}) - h(\tilde{\theta}, \tilde{z})) &= \\ &= \begin{pmatrix} \theta \\ 1-\theta \end{pmatrix} \cdot \begin{pmatrix} \tilde{\theta}-\theta \\ \theta-\tilde{\theta} \end{pmatrix} + \begin{pmatrix} \tilde{\theta} \\ 1-\tilde{\theta} \end{pmatrix} \cdot \begin{pmatrix} \theta-\tilde{\theta} \\ \tilde{\theta}-\theta \end{pmatrix} \\ &= -2(\theta-\tilde{\theta})^2 \\ &= -\left\| \begin{pmatrix} \theta \\ 1-\theta \end{pmatrix} - \begin{pmatrix} \tilde{\theta} \\ 1-\tilde{\theta} \end{pmatrix} \right\|^2 .\end{aligned}$$

Since Assumption 2 above fails, the result of Gomes et al. [7] giving uniqueness does not apply. Nevertheless, solutions to the initial-terminal value problem (ITVP) given by (3.1) are unique as will be shown. As the goal is to understand θ not u, a simplification of (3.1) can be used. Let $y = u_1 - u_0$. Then by (3.1)

$$\begin{aligned}-\dot{y} &= -\dot{u}_1 + \dot{u}_0 \\ &= 1 - 2\theta - \frac{1}{2}y_+^2 + \frac{1}{2}(-y)_+^2 \\ &= 1 - 2\theta - \frac{1}{2}y|y|.\end{aligned}$$

Also let $x = 2\theta - 1$ and so $x_0 = 2\bar{\theta} - 1$. Then

$$\begin{aligned}\dot{x} &= 2\dot{\theta} \\ &= 2(1-\theta)y_+ - 2\theta(-y)_+ \\ &= -(x-1)y_+ - (x+1)(-y)_+ \\ &= y - x|y|.\end{aligned}$$

The following system is analyzed in place of (3.1), where $\theta = \frac{1+x}{2}$

$$\begin{cases} -\dot{y} = -x - \dfrac{1}{2}y|y|, & y(T) = 0 \\ \dot{x} = y - x|y|, & x(0) = x_0 \in [-1, 1]. \end{cases} \tag{3.2}$$

The associated TVP allows for finding solutions which guarantee that $y(T) = 0$, which must always be true. For convenience look at time in reverse from T, that is to map $t \mapsto T - t$. Moving backwards and with initial conditions and forgetting the condition x_0, then (3.2) becomes

$$\begin{cases} \dot{y} = -x - \dfrac{1}{2}y|y|, & y(0) = 0 \\ \dot{x} = -y + x|y|, & x(0) = \epsilon \in [-1, 1]. \end{cases} \tag{3.3}$$

If (x, y) solved (3.3) then $\ddot{y} = -\dot{x} - \dot{y}|y| = y - x|y| + x|y| + \frac{1}{2}y^3 = y + \frac{1}{2}y^3$. So y solves the following with $\dot{y}(0) = x(0)$

$$\begin{cases} \dot{y} = v, & y(0) = 0 \\ \dot{v} = y + \dfrac{1}{2}y^3, & v(0) = \epsilon \in [0, 1]. \end{cases} \tag{3.4}$$

Local Lipschitz continuity of the right-hand side of (3.3) implies uniqueness, given a time interval where solutions are bounded. Time intervals so that solutions to (3.3) blow up are not considered, because in (3.2) the only interest is for solutions (x, y) such that $x \in [-1, 1]$, and y cannot blow up while x is bounded.

Lemma 3.1.1. *Suppose (x_1, y_1) and (x_2, y_2) solve* (3.3) *with $x_1(0) > x_2(0) \in [-1, 1]$. Suppose that neither solution blows up on $[0, \tau]$. Then $x_1 > x_2$ on $[0, \tau]$.*

Proof. Assume (x_1, y_1) and (x_2, y_2) solve (3.3) with $x_1(0) > x_2(0) \in [-1, 1]$, and that neither solution blows up on $[0, \tau]$. Then $(y_i, \dot{y}_i)$ solves (3.4), where $\dot{y}_i(0) = -x_i(0)$ for $i = 1, 2$. It will be shown that $y_1(t) < y_2(t)$ for $t \in [0, \tau]$ first, then that $x_1 > x_2$.

First note that $\dot{y}_2(0) = x_2(0) > x_1(0) = \dot{y}_1(0)$. Suppose there exists a $t^* \in [0, \tau]$ so

that $y_2(t^*) = y_1(t^*)$ and $y_2(t) > y_1(t)$ for any $t \in (0, t^*)$. Then by (3.4), $\ddot{y}_2(t) > \ddot{y}_1(t)$ for any $t \in (0, t^*)$, and thus $\dot{y}_2(t) - \dot{y}_1(t) > \dot{y}_2(0) - \dot{y}_1(0) > 0$ for any $t \in (0, t^*)$. Then $y_2(t^*) - y_1(t^*) > y_2(0) - y_1(0) = 0$, a contradiction. Therefore $y_2(t) > y_1(t)$, and hence $\dot{y}_2(t) > \dot{y}_1(t)$ for $t \in [0, \tau]$.

Since $y|y|$ is an increasing function, $y_1|y_1| < y_2|y_2|$. By (3.3), $-x_i = \dot{y}_i + \frac{1}{2} y_i|y_i|$. Therefore one has $-x_1 = \dot{y}_1 + \frac{1}{2} y_1|y_1| < \dot{y}_2 + \frac{1}{2} y_2|y_2| = -x_2$, hence $x_1 > x_2$ for $t \in [0, \tau]$ (see Fig. 3.1 for intuition). □

The following theorem immediately follows.

Theorem 3.1.2. *System* (3.2) *with* $x_0 \in [-1, 1]$ *for a given time to play* $T > 0$ *has a unique solution.*

Proof. Suppose that (x_1, y_1) and (x_2, y_2) solve (3.2) with $x_1(0) = x_2(0) \in [-1, 1]$ and are bounded on $[0, T]$. Suppose that $x_1(T) > x_2(T)$, then by Lemma 3.1.1 $x_1(t) > x_2(t)$ for $t \in [0, T]$, but this contradicts that $x_1(0) = x_2(0)$. Same for $x_1(T) < x_2(T)$.

Suppose that $x_1(T) = x_2(T)$. Since (3.2) is locally Lipschitz and $y_1(T) = y_2(T)$, $x_1 \equiv x_2$ on $[0, T]$. Hence the conclusion. □

3.2 Introduction to 2-State Follow the Crowd Case

In this section a case of follow the crowd for two states is introduced and some basic properties are discussed. In particular, uniqueness of solutions to this MFG model does not hold; see Fig. 2.1. Assume that the running cost is $c(i, \theta, \alpha) = |1 - i - \theta| + \alpha_{i,1-i}^2/2$. For this running cost function, (2.18) becomes

$$\begin{cases} -\dot{u}_0 = 1 - \theta - \dfrac{1}{2}(u_0 - u_1)_+^2 \\ -\dot{u}_1 = \theta - \dfrac{1}{2}(u_1 - u_0)_+^2 \\ \dot{\theta} = -\theta(u_0 - u_1)_+ + (1 - \theta)(u_1 - u_0)_+ \\ u_i(T) = 0, \theta(0) = \bar{\theta}. \end{cases} \tag{3.5}$$

As in the previous section, the goal is to understand θ, and (as with the avoid the crowd cost) (3.5) is simplified by assuming $y = u_1 - u_0$ and $x = 2\theta - 1$. System (3.5) yields

$$\begin{aligned} -\dot{y} &= -\dot{u}_1 + \dot{u}_0 \\ &= 2\theta - 1 - \frac{1}{2}y_+^2 + \frac{1}{2}(-y)_+^2 \\ &= x - \frac{1}{2}y|y|, \end{aligned}$$

and

$$\begin{aligned} \dot{x} &= 2\dot{\theta} \\ &= 2(1-\theta)y_+ - 2\theta(-y)_+ \\ &= -(x-1)y_+ - (x+1)(-y)_+ \\ &= y - x|y|. \end{aligned}$$

Thus (3.5) simplifies to

$$\begin{cases} -\dot{y} = x - \frac{1}{2}y|y|, & y(T) = 0 \\ \dot{x} = y - x|y|, & x(0) = x_0 \in [-1, 1]. \end{cases} \tag{3.6}$$

Suppose that $y(t) \geq 0$ on $t \in [0, T]$. Then

$$\begin{aligned} &\frac{dx}{dt}(t) = y(1-x)(t) \\ &\implies d[-\ln(1-x)](t) = y(t)dt \\ &\implies -\ln(1-x(t)) + \ln(1-x(0)) = \int_0^t y(r)dr \\ &\implies \frac{1-x(t)}{1-x(0)} = e^{-\int_0^t y(r)dr}. \end{aligned} \tag{3.7}$$

Likewise $\frac{1+x(t)}{1+x(0)} = e^{\int_0^t y(r)dr}$ if $y(t) \leq 0$ on $t \in [0, T]$.

The conditions in Gomes et al. [7] for uniqueness of solutions to (3.6) again are considered. In addition to Assumption 2 failing as before, Assumption 3 also fails. Recall that

$$h(\theta, z) = \begin{pmatrix} 1 - \theta - \frac{1}{2}(z_0 - z_1)_+^2 \\ \theta - \frac{1}{2}(z_1 - z_0)_+^2 \end{pmatrix},$$

and that Assumption 3 of the monotonicity conditions required that for $\theta, \tilde{\theta} \in [0, 1]$ and $\gamma > 0$

$$\begin{pmatrix} \theta \\ 1 - \theta \end{pmatrix} \cdot (h(\tilde{\theta}, z) - h(\theta, z)) + \begin{pmatrix} \tilde{\theta} \\ 1 - \tilde{\theta} \end{pmatrix} \cdot (h(\theta, \tilde{z}) - h(\tilde{\theta}, \tilde{z})) \leq -\gamma \left\| \begin{pmatrix} \theta \\ 1 - \theta \end{pmatrix} - \begin{pmatrix} \tilde{\theta} \\ 1 - \tilde{\theta} \end{pmatrix} \right\|^2.$$

System (3.6) fails that condition because

$$\begin{aligned} \begin{pmatrix} \theta \\ 1 - \theta \end{pmatrix} \cdot (h(\tilde{\theta}, z) - h(\theta, z)) + \begin{pmatrix} \tilde{\theta} \\ 1 - \tilde{\theta} \end{pmatrix} \cdot (h(\theta, \tilde{z}) - h(\tilde{\theta}, \tilde{z})) &= \\ = \begin{pmatrix} \theta \\ 1 - \theta \end{pmatrix} \cdot \begin{pmatrix} \theta - \tilde{\theta} \\ \tilde{\theta} - \theta \end{pmatrix} + \begin{pmatrix} \tilde{\theta} \\ 1 - \tilde{\theta} \end{pmatrix} \cdot \begin{pmatrix} \tilde{\theta} - \theta \\ \theta - \tilde{\theta} \end{pmatrix} & \\ = 2(\theta - \tilde{\theta})^2 & \\ > -\gamma 2(\theta - \tilde{\theta})^2 & \\ = -\gamma \left\| \begin{pmatrix} \theta \\ 1 - \theta \end{pmatrix} - \begin{pmatrix} \tilde{\theta} \\ 1 - \tilde{\theta} \end{pmatrix} \right\|^2. & \end{aligned}$$

In Chapter 2 the plot in Fig. 2.1 showed two solutions to the (3.5) with the same boundary conditions. Understanding of the non-unique solutions x to (3.6) will be covered in the next section.

3.3 Non-Uniqueness Analysis of Follow the Crowd via TVP

The goal in this section is the proof of Theorem 3.3.1 below, which gives the number of solutions to (3.5) given $\bar{\theta} = \frac{1}{2}$ and time to play T. The interest of $\bar{\theta} = \frac{1}{2}$ is due to the fact that all non-constant solutions to (3.3) always eventually pass through $\frac{1}{2}$; see Lemma 3.3.7.

Theorem 3.3.1. *System* (3.5) *with* $\theta(0) = \frac{1}{2}$ *and positive time to play* $T \in (\frac{\pi}{2} + (k-1)\pi, \frac{\pi}{2} + k\pi]$ *for* $k \in \mathbb{N}_0$, *has exactly* $1 + 2k$ *solutions.*

This section contains lemmas leading up to the proof of Theorem 3.3.1. Along the way it is shown the solutions are periodic, after being analytically extended from $[0, T]$ to $\mathbb{R}$. There are monotonicity results of the solutions to (3.6) which are used in showing the number of solutions to (3.5) is increasing (given $\theta(0) = 1/2$) in T. There is a further continuity result which ensures that the number of solutions to (3.5) are increasing in a predictable way. However, the most important result leading to Theorem 3.3.1, is Lemma 3.3.16 which gives an asymptotic of a solution to (3.5) on a set.

The initial-terminal conditions given for (3.6) make it difficult to solve. Instead the condition $x(0) = x_0$ is dropped and a value for $x(T)$ is chosen, running the ODE backwards in time. By symmetry of the cost functions over the states, it may be assumed that $x(T)$ is non-negative, and since $x(T) \in \{0, 1\}$ gives that x is constant, it may be assumed that $x(T) \in (0, 1)$. To simplify the ODE substitute $t \mapsto T - t$. Then (3.6) becomes

$$\begin{cases} \dot{x} = -y + x|y|, x(0) \in [0, 1] \\ \dot{y} = x - \dfrac{1}{2}y|y|, y(0) = 0. \end{cases} \tag{3.8}$$

Definition 3.3.2. *Consider the family of solution pairs* (x_ϵ, y_ϵ) *which solves* (3.8) *given initial condition* $x_\epsilon(0) = \epsilon$. *Define the function* $\tau_X : (0, 1) \to \mathbb{R}^+$ *so that* $\tau_X(\epsilon) = \inf\{t \geq 0 : x_\epsilon(t) = 0\}$ *for any* $\epsilon \in (0, 1)$. *Define the function* $\tau_Y : (0, 1) \to \mathbb{R}^+$ *so that* $\tau_Y(\epsilon) = \inf\{t > 0 : y_\epsilon(t) = 0\}$ *for any* $\epsilon \in (0, 1)$.

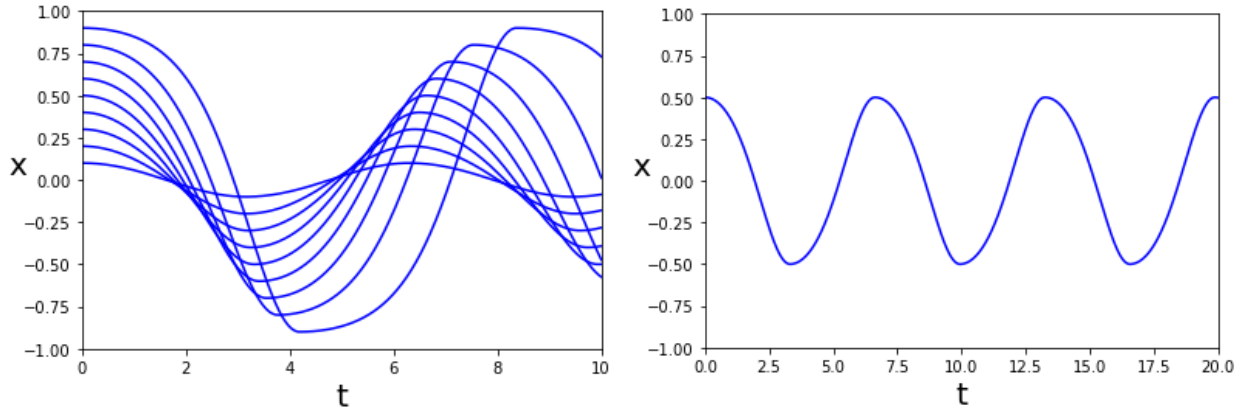

Figure 3.2: On the left are many solutions with various IC to (3.8). The solutions overlap, indicating that there are non-unique solutions to (3.6). On the right the periodicity is illustrated for one such solution, for $T = 20$.

It is not immediately obvious that τ_X, τ_Y are finite (hence well-defined), but this is shown in Lemmas 3.3.8 and 3.3.9. Over the course of this section the following theorem is shown.

Theorem 3.3.3. *The functions $\tau_X, \tau_Y : (0,1) \to \mathbb{R}^+$ are continuous and monotonically increasing. They are bijective onto $(\frac{\pi}{2}, \infty)$ and (π, ∞) respectively.*

Figure 3.2 indicates the periodicity of (3.8) and that the solutions can cross each other indicating non-uniqueness of the ITVP. Analysis of (3.8) will shed light on the nature of solutions to (3.5). Nevertheless, even (3.8) is not trivial to analyze.

An important observation is that y, where (x, y) solves (3.8), can be solved independently of x. Consider the second derivative of y from (3.8),

$$\begin{aligned}\ddot{y} &= \dot{x} - |y|\dot{y} \\ &= -y + x|y| - |y|\left(x - \frac{1}{2}y|y|\right) \\ &= -y + \frac{1}{2}y^3 \text{ and } \dot{y}(0) = x(0).\end{aligned}$$

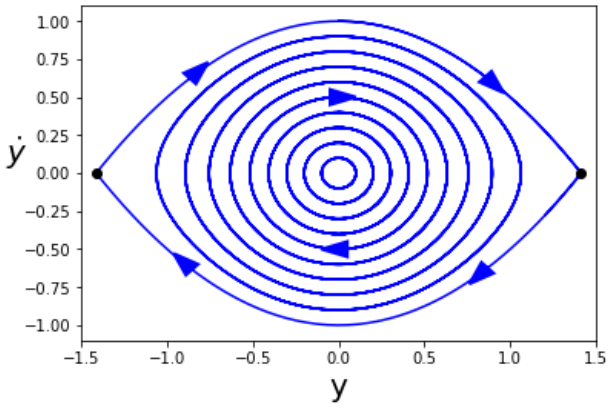

Figure 3.3: The phase plane for (3.9).

Then a solution (x, y) to (3.8) is such that y solves the following ODE with $\dot{y}(0) = x(0)$,

$$\begin{cases} \ddot{y} = -y + \frac{1}{2}y^3 \\ y(0) = 0, \dot{y}(0) = \epsilon \in [0, 1]. \end{cases} \tag{3.9}$$

The ODE given by (3.9) is well understood, see Fig. 3.3 for the phase plane, and may be posed as a first-order system

$$\begin{cases} \dot{y} = v, & y(0) = 0 \\ \dot{v} = -y + \frac{1}{2}y^3, & v(0) = \epsilon \in [0, 1]. \end{cases} \tag{3.10}$$

Let

$$H(y, v) = \frac{1}{2}y^2 - \frac{1}{8}y^4 + \frac{1}{2}v^2. \tag{3.11}$$

Then H is the Hamiltonian for the dynamics given by (3.10). In other words, $\dot{y} = H_v$ and $\dot{v} = -H_y$. It follows that H is constant along solutions of the ODE.

Lemma 3.3.4. *If (y, v) solves* (3.10) *then $|y| \leq \sqrt{2}$ and $|v| \leq \epsilon$.*

Proof. Let $v(0) = \epsilon \in [0, 1]$. Consider the level set of the Hamiltonian which contains the point $(0, \epsilon)$. The value of the Hamiltonian on this level set is $H(0, \epsilon) = \frac{1}{2}\epsilon^2$. Then the level

set is given by

$$\frac{1}{2}\epsilon^2 = H(y,v) = \frac{1}{2}y^2 - \frac{1}{8}y^4 + \frac{1}{2}v^2$$
$$\text{or } y^2(y^2-4) = 4(v^2-\epsilon^2). \tag{3.12}$$

Recall that $y(0) = 0$ and $v(0) = \epsilon$. Suppose that there exists $t > 0$ so that $y(t) = \sqrt{2}$. Then the left-hand side of (3.12) is -4, but then $-4 = 4(v^2 - \epsilon^2)$ or $v^2 = -1 + \epsilon^2$ which is a contradiction because $|\epsilon| < 1$. Thus $y(t) \neq \sqrt{2}$ for all t. Likewise $y(t) \neq -\sqrt{2}$ for all t. Therefore $|y| < \sqrt{2}$ for all $t > 0$ because of the IC $y(0) = 0$. Moreover, this means the left-hand side of (3.12) is always non-positive hence $|v| \leq \epsilon$. □

Lemma 3.3.5. *If (y,v) solves* (3.10) *with $v(0) = \epsilon \in [0,1]$, then $|y| = \sqrt{2(1-\sqrt{v^2+1-\epsilon^2})}$.*

Proof. Since the Hamiltonian is constant along the solution

$$\begin{aligned}
&H(y,v) = \frac{1}{2}\epsilon^2 = \frac{1}{2}y^2 - \frac{1}{8}y^4 + \frac{1}{2}v^2 \\
&\iff 4v^2 = y^4 - 4y^2 + 4\epsilon^2 = \left(y^2-2\right)^2 - \left(2\sqrt{1-\epsilon^2}\right)^2 \\
&\implies 2 - y^2 = \sqrt{4v^2 + \left(2\sqrt{1-\epsilon^2}\right)^2} = 2\sqrt{v^2+1-\epsilon^2} \text{ because } |y| < \sqrt{2} \text{ by Lemma 3.3.4.} \\
&\iff |y| = \sqrt{2(1-\sqrt{v^2+1-\epsilon^2})}.
\end{aligned}$$

□

Remark 3.3.6. *Assume that (x,y) solves* (3.8)*. Then y solves* (3.9) *and $(y,\dot{y})$ solves* (3.10)*. A point is a fixed point of* (3.10) *if and only if $(\dot{y},\dot{v}) = (0,0)$. The zeros of $-y + \frac{1}{2}y^3$ are $y = 0, \pm\sqrt{2}$. Thus there are three fixed points $\{(\pm\sqrt{2},0),(0,0)\}$. The Jacobian of the right-hand side of* (3.10) *at a point (y,v) is*

$$J_{(y,v)} = \begin{pmatrix} 0 & 1 \\ \frac{3}{2}y^2 - 1 & 0 \end{pmatrix}$$

so its eigenvalues satisfy $\lambda^2 - (\frac{3}{2}y^2 - 1) = 0$. For the fixed points $(\pm\sqrt{2},0)$ are saddles because

the Jacobian has eigenvalues $\lambda = \pm\sqrt{2}$. For the fixed point $(0,0)$ the Jacobian has eigenvalues $\lambda = \pm i$, thus the origin being stable of concentric orbits.

3.3.1 Prerequisite Properties of τ_X and τ_Y

Throughout this section basic properties of the functions x, y, τ_X and τ_Y are discovered where (x, y) solves (3.8). The following lemma is given to classify the end point cases as well as the majority case, for the IC.

Lemma 3.3.7. *Suppose that y solves* (3.9)*. If $\dot{y}(0) = 0$ then $y \equiv 0$. If $\dot{y}(0) = 1$ then y is monotonic. If $\dot{y}(0) = \epsilon \in (0,1)$ then y has a local max.*

Proof. Assume y solves (3.9) with $\dot{y}(0) = \epsilon \in [0,1]$. Let $v = \dot{y}$.

If $\epsilon = 0$ then by uniqueness $y \equiv 0$.

If $\epsilon = 1$, then $v(0) = 1$ and by Lemma 3.3.5 $y^2 = 2 - 2|v|$, which contains the fixed points $(\pm\sqrt{2}, 0)$, see Remark 3.3.6. Thus y converges to either $\pm\sqrt{2}$. In the first quadrant of the phase plane y increases, and by Lemma 3.3.4 $y < \sqrt{2}$ so v decreases. Thus y is monotonically increasing and $y \to \sqrt{2}$ as $t \to \infty$.

Suppose that $\epsilon \in (0,1)$. Then by Lemma 3.3.5, $|y| = \sqrt{2(1 - \sqrt{v^2 + 1 - \epsilon^2})}$. Whenever $v = 0$, $|y| = \sqrt{2(1 - \sqrt{1 - \epsilon^2})} < \sqrt{2}$. Thus y has no fixed point, and so y does not converge. But since y is bounded it must not be monotone and hence must have a local max. □

There are many straightforward properties of a solution y, such as periodicity, multiple symmetries, and their signed regions. These are covered in the following lemma.

Lemma 3.3.8. *Suppose that y solves* (3.9) *with IC $\dot{y}(0) = \epsilon \in (0,1)$. Then y attains its first local max at $\frac{\tau_Y(\epsilon)}{2}$. Furthermore $y\left(\frac{\tau_Y(\epsilon)}{2} + t\right) = y\left(\frac{\tau_Y(\epsilon)}{2} - t\right)$ for $t \in \left[0, \frac{\tau_Y(\epsilon)}{2}\right]$, $y(t) = -y\left(\tau_Y(\epsilon) + t\right)$ for $t \geq 0$, and y has period $2\tau_Y(\epsilon)$. Finally, $y(t) > 0$ for $t \in (0, \tau_Y(\epsilon))$ and $y(t) < 0$ for $t \in (\tau_Y(\epsilon), 2\tau_Y(\epsilon))$.*

Proof. Let $T > 0$ be the first time that y attains a local max. It will eventually be shown that $T = \frac{\tau_Y(\epsilon)}{2}$, but first the properties of y will be shown using time T. By Lemma 3.3.7,

$T < \infty$. Note that solutions to (3.9) are unique, because y is bounded by Lemma 3.3.4 and hence Lipschitz conditions apply. Define w_+, w_- for $t \in [0, T]$ so that $w_+(t) = y(T + t)$ and $w_-(t) = y(T - t)$. Then

$$\begin{aligned} \ddot{w}_+(t) &= \ddot{y}(T+t) & & & \ddot{w}_-(t) &= \ddot{y}(T-t) \\ w_+(0) &= y(T) & & \text{and} & w_-(0) &= y(T) \\ \dot{w}_+(0) &= \dot{y}(T) = 0 & & & \dot{w}_-(0) &= -\dot{y}(T) = 0. \end{aligned}$$

Since solutions to (3.9) are unique and $w_+ - w_-$ solves (3.9) with $\epsilon = 0$, $w_+ \equiv w_-$. Thus $y(T + t) = y(T - t)$ for $t \in [0, T]$. This implies that $y(2T) = y(0) = 0$, or that $\tau_Y(\epsilon) \leq 2T$.

Define z for $t \in [0, 2T]$ so that $z(t) = -y(2T + t)$. Then

$$\ddot{z}(t) = -\ddot{y}(2T+t) = -\left(-y(2T+t) + \frac{1}{2}y(2T+t)^3\right) = -z(t) + \frac{1}{2}z(t)^3,$$

$z(0) = -y(2T) = 0$ and $\dot{z}(0) = -\dot{y}(2T) = -\dot{w}_+(T) = -\dot{w}_-(T) = \dot{y}(0)$. Thus $y \equiv z$, or $y(t) = -y(2T + t)$. Furthermore, $y(t) = -y(2T + t) = y(4T + t)$ for $t \geq 0$, so y has period $4T$.

Since $\dot{y}(0) > 0$ and by definition of T, $\dot{y}(t) \geq 0$ for $t \in [0, T]$. So $y(t) \geq 0$ for $t \in [0, T]$. But since $y(T + t) = y(T - t)$ for $t \in [0, T]$, it is in fact the case that $y(t) > 0$ for $t \in (0, 2T)$. Thus $T = \frac{\tau_Y(\epsilon)}{2}$. Hence the conclusion, because $y(t) < 0$ for $t \in (\tau_Y(\epsilon), 2\tau_Y(\epsilon))$ since $y(t) = -y(2T + t)$ for $t \geq 0$. □

Note that the Lemma 3.3.8 is obvious by the symmetries of the Hamiltonian given by (3.11), and the proof above is simply an elaboration of this fact. Likewise the coordinate x of (3.8) has properties of periodicity, symmetry, and regions of monotonicity.

Lemma 3.3.9. *Suppose that (x, y) solves* (3.8) *with $x(0) = \epsilon \in (0, 1)$. Then $x(t) = -x(t+\tau_Y(\epsilon))$, $\tau_X < \tau_Y$ and x and y have the same period $2\tau_Y(\epsilon)$. Finally, x is strictly decreasing on $(0, \tau_Y(\epsilon))$ and strictly increasing on $(\tau_Y(\epsilon), 2\tau_Y(\epsilon))$.*

Proof. Lemma 3.3.8 applies and so y is periodic, with period $2\tau_Y(\epsilon)$. Also by Lemma 3.3.8

$$x(t) = \dot{y}(t) + \frac{1}{2}y(t)|y(t)| = -\dot{y}(t + \tau_Y(\epsilon)) - \frac{1}{2}y(t + \tau_Y(\epsilon))|y(t + \tau_Y(\epsilon))| = -x(t + \tau_Y(\epsilon)). \tag{3.13}$$

Thus $x(t) = -x(t + \tau_Y(\epsilon)) = x(t + 2\tau_Y(\epsilon))$ and so x is periodic with period at most $2\tau_Y(\epsilon)$. Also $\tau_X(\epsilon) < \tau_Y(\epsilon)$ since $x(0) = -x(\tau_Y(\epsilon))$.

By Lemma 3.3.8, y is positive on $(0, \tau_Y(\epsilon))$. Since $\dot{x} = -y + x|y| = -y(1 - x) < 0$ on $(0, \tau_Y(\epsilon))$. Also $\dot{x} > 0$ on $(\tau_Y(\epsilon), 2\tau_Y(\epsilon))$ since $x(t) = -x(t + \tau_Y(\epsilon))$. Thus x is strictly decreasing on $(0, \tau_Y(\epsilon))$ and x is strictly increasing on $(\tau_Y(\epsilon), 2\tau_Y(\epsilon))$. Therefore x has period $2\tau_Y(\epsilon)$. □

The following remark shows convexity of the Hamiltonian's contours, and gives an implication.

Remark 3.3.10. *Consider a solution to* (3.9) *with IC* $\epsilon \in (0, 1)$. *Suppose that* $t \in \left(0, \frac{\tau_Y(\epsilon)}{2}\right)$, *then by Lemma 3.3.8 both* $y(t), \dot{y}(t) \geq 0$ *and by Lemma 3.3.4* $|y| < \sqrt{2}$, *so the slope of the curve in the phase plane is*

$$\frac{d\dot{y}}{dy} = \frac{\ddot{y}}{\dot{y}} = \frac{-y + \frac{1}{2}y^3}{\dot{y}}, \tag{3.14}$$

which is negative and decreasing as y *increases and as* $\dot{y}$ *decreases, hence the concavity of the curve in the phase plane for* $t \in \left(0, \frac{\tau_Y(\epsilon)}{2}\right)$. *That is by* (3.14), *if* $t_1, t_2 \in (0, \tau_Y(\epsilon))$ *with* $t_1 < t_2$ *then*

$$\frac{d\dot{y}}{dy}(t_1) > \frac{d\dot{y}}{dy}(t_2)$$

or

$$0 > \frac{d\dot{y}}{dy}(t_1) \geq \frac{\dot{y}(t_2) - \dot{y}(t_1)}{y(t_2) - y(t_1)}. \tag{3.15}$$

Equation (3.15) is eventually used to find the upper bound $\lim_{\epsilon \to 0+} \tau_Y(\epsilon) \leq \pi$. The lower

bound of τ_Y is found in the following lemma.

Lemma 3.3.11. *For any ϵ, $\tau_Y(\epsilon) > \pi$.*

Proof. Consider a solution y to (3.9) with IC $\epsilon \in (0,1)$. Suppose that $t \in (0, \tau_Y(\epsilon))$, then by Lemma 3.3.8, $y(t), \dot{y}(t) \geq 0$. The angle at $(y, \dot{y})$ as a function of time defined by

$$\theta := \arctan\left(\frac{\dot{y}}{y}\right),$$

satisfies

$$\dot{\theta} = \frac{1}{1+(\frac{\dot{y}}{y})^2}\frac{\ddot{y}y - \dot{y}\dot{y}}{y^2} = \frac{\left(-y+\frac{1}{2}y^3\right)y - \dot{y}\dot{y}}{\dot{y}^2+y^2} = -1 + \frac{1}{2}\frac{y^4}{\dot{y}^2+y^2}. \tag{3.16}$$

Thus $\theta(t) \geq \theta(0) + \int_0^t -1 ds = \frac{\pi}{2} - t$, and so $\theta(t) \geq 0$ for $t \in [0, \pi/2]$. This means that the first local max happens for some $t \geq \frac{\pi}{2}$. Thus by Lemma 3.3.8, $\tau_Y(\epsilon) > \pi$. □

The next result gives a monotonicity of the solutions (x, y) to (3.8) with respect to the IC, see Fig. 3.4.

Theorem 3.3.12. *Let (x_1, y_1) and (x_2, y_2) be solutions to* (3.8) *with IC $x_1(0) = \epsilon_1$ and $x_2(0) = \epsilon_2$ in $(0,1)$ with $x_1(0) < x_2(0)$. Then $y_1(t) < y_2(t)$ for $t \in (0, \tau_Y(\epsilon_1))$. Moreover $x_1(t) < x_2(t)$ for $t \in [0, \tau_X(\epsilon_1)]$.*

Proof. Recall that $y_1(t), \dot{y}_1(t) > 0$ for $t \in (0, \tau_Y(\epsilon_1)/2)$, by Lemma 3.3.8. Define the functions $\theta_1 = \arctan(\frac{\dot{y}_1}{y_1})$ and $\theta_2 = \arctan(\frac{\dot{y}_2}{y_2})$.

Then $\dot{\theta}_1 = -1 + \frac{1}{2}\frac{y_1^2}{1+\left(\frac{\dot{y}_1}{y_1}\right)^2}, \dot{\theta}_2 = -1 + \frac{1}{2}\frac{y_2^2}{1+\left(\frac{\dot{y}_2}{y_2}\right)^2}$; see (3.16). Taking a limit gives $\dot{\theta}_1(0) < \dot{\theta}_2(0)$. Suppose that $\theta_1(t^*) = \theta_2(t^*)$ and $\theta_1(t) < \theta_2(t)$ for $t \in (0, t^*)$ for some $t^* \in \left(0, \frac{\tau_Y(\epsilon_1)}{2}\right]$, then $\dot{\theta}_1(t^*) \geq \dot{\theta}_2(t^*)$. Proceed by contradiction. By definition $\theta_1 = \theta_2$ implies that $\frac{\dot{y}_1}{y_1} = \frac{\dot{y}_2}{y_2}$. Since $\theta_1 = \theta_2$, at t^*, the distance from the origin of these points are such that $y_1^2 + \dot{y}_1^2 < y_2^2 + \dot{y}_2^2$, else the Hamiltonian level sets would be crossing. Those facts together give $y_2 > y_1$ (similar

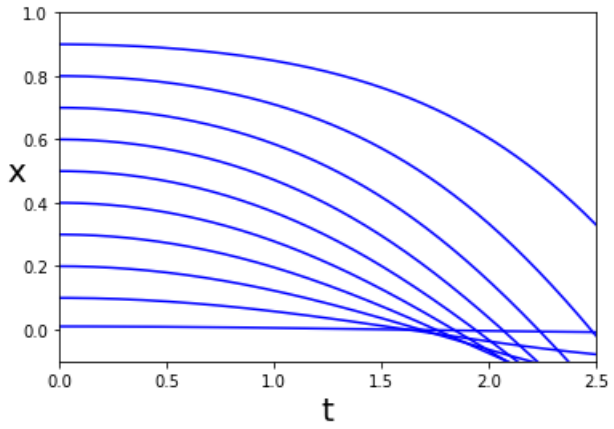

Figure 3.4: Many instances of x with different TC.

triangles). So

$$\dot{\theta}_1(t^*) = -1+\frac{1}{2}\frac{y_1^2}{1+\left(\frac{\dot{y}_1}{y_1}\right)^2} = -1+\frac{1}{2}\frac{y_1^2}{1+\left(\frac{\dot{y}_2}{y_2}\right)^2} < -1+\frac{1}{2}\frac{y_2^2}{1+\left(\frac{\dot{y}_2}{y_2}\right)^2} = \dot{\theta}_2(t^*), \text{ a contradiction.}$$

Thus $\theta_1(t) < \theta_2(t)$ for $t \in \left(0, \frac{\tau_Y(\epsilon_1)}{2}\right]$ and hence $y_1(t) < y_2(t)$ for $t \in \left(0, \frac{\tau_Y(\epsilon_1)}{2}\right]$. Moreover by Lemma 3.3.8 $y_i(t) = y_i(\tau_Y(\epsilon_i) - t)$, hence $y_1(t) = y_1(\tau_Y(\epsilon_1) - t) < y_2(\tau_Y(\epsilon_1) - t) < y_2(\tau_Y(\epsilon_2) - t) = y_2(t)$ for $t \in \left[\frac{\tau_Y(\epsilon_1)}{2}, \tau_Y(\epsilon_1)\right)$. Thus $y_1(t) < y_2(t)$ for $t \in (0, \tau_Y(\epsilon_1))$.

It was shown that $0 \leq y_1 < y_2$, so the inequality $\dot{x}_2 = y_2(x_2 - 1) > y_1(x_2 - 1)$ holds for $t \in (0, \tau_Y(\epsilon))$. Since $\tau_X(\epsilon) < \tau_Y(\epsilon)$, if $x_1 = x_2$ then $\dot{x}_2 > y_1(x_2 - 1) = \dot{x}_1$ for $\forall t \in [0, \tau_X(\epsilon_1)]$. Hence $x_2 > x_1$ for $\forall t \in [0, \tau_X(\epsilon_1)]$ (see Fig. 3.4 for the intuition). □

The following is immediate, but is stated separately for convenience.

Corollary 3.3.13. *The functions τ_X, τ_Y are monotonically increasing.*

Proof. Immediate from the conclusion of Theorem 3.3.12. □

Since the solutions (x, y) to (3.8) for $x(0) = \epsilon \in (0, 1)$ cross the horizontal axis non-tangentially, as opposed to touching it at a point and then retreating (or "kissing the axis"), the functions τ_X, τ_Y are continuous.

Lemma 3.3.14. *The functions τ_X, τ_Y are continuous.*

Proof. Suppose there is a sequence of solutions (x_n, y_n) to (3.8) and some solution (x, y) to that system, so that the sequence of initial values $x_n(0) \in [0, 1]$ converges from above to some initial value $x(0) \in [0, 1]$. By Lemmas 3.3.8 and 3.3.9 $\dot{x}(\tau_X(x(0))), \dot{y}(\tau_Y(x(0))) < 0$.

Fix $\delta > 0$. For simplicity let $\tau = \tau_X(x(0))$. The proof will show that τ_X is continuous; the argument for τ_Y is similar. Since $\dot{x}(\tau) < 0$ and $x(\tau) = 0$, for δ sufficiently small $x(\tau+\delta) < 0$. Then by the Lipschitz conditions x_n converges to x, thus there exists an $N \in \mathbb{N}$ so that $\forall n > N$, $x_n(\tau + \delta) < 0$, because $x(\tau + \delta) < 0$. Therefore for $n > N$, $\tau_X(x_n(0)) < \tau + \delta$ and by Corollary 3.3.13 $\tau < \tau_X(x_n(0))$. Since δ was arbitrary, $\lim_{n\to\infty} \tau_X(x_n(0)) = \tau$. The same holds for sequences $x_n(0)$ converges from below to $x(0)$. Thus τ_X is continuous. □

The remainder of the proof of Theorem 3.3.3 is shown in Section 3.3.3. The next section relates to bounding x and y for a short time. Theorem 3.3.1 is proved in Section 3.3.4.

3.3.2 Bounding Asymptotic Solutions

In this section bounds for the solution (x, y) to (3.8) for $x(0) = \epsilon$ are derived on subsets of their domain. Having such bounds for our solutions will allow for an argument of asymptotic solution for small choices of ϵ. These results will assist in finding the ranges of τ_X, τ_Y in the next section. The following remark gives intuition about the solutions y for small ϵ.

Remark 3.3.15. *Recall* (3.8),

$$\begin{cases} \dot{x} = -y + x|y|, x(0) = \epsilon \in [0, 1] \\ \dot{y} = x - \dfrac{1}{2}y|y|, y(0) = 0. \end{cases}$$

Letting $\tilde{x} = x/\epsilon$ and $\tilde{y} = y/\epsilon$, the above equation becomes

$$\begin{cases} \dot{\tilde{x}} = -\tilde{y} + \epsilon\tilde{x}|\tilde{y}|, \tilde{x}(0) = 1, \\ \dot{\tilde{y}} = \tilde{x} - \dfrac{\epsilon}{2}\tilde{y}|\tilde{y}|, \tilde{y}(0) = 0. \end{cases}$$

In the limit $\epsilon \to 0$, the solution is $\tilde{y}(t) = \sin(t)$. Thus $y(t) = \epsilon \sin(t) + o(\epsilon)$, but this is not enough to determine the lower bound of τ_Y. Theorem 3.3.1 can not be proven without knowing the codomains of τ_X and τ_Y.

In consideration of Remark 3.3.15, suppose y solves (3.9) for a particular $\epsilon \in (0, 1)$. Let $z(t) := y(t) - \epsilon \sin(t)$. Then

$$\begin{cases} \ddot{z} = -z + \dfrac{1}{2}(z + \epsilon \sin(t))^3 \\ z(0) = 0, \dot{z}(0) = 0. \end{cases} \tag{3.17}$$

Bounds for z give bounds for y, and bounds for z will be found.

Lemma 3.3.16. *Let z be a solution to* (3.17)*. Then $0 \leq z(t) < .3\epsilon^3 \sin(t)$ for $t \in [0, \pi/2]$.*

Proof. Let τ be the first strictly positive time such that $\ddot{z}(\tau) = 0$. First a bound for $z(t)$ on $t \in [0, \tau]$ is found, then $\tau > \pi/2$ is shown. Since $z(0) = 0$, by (3.17) $\ddot{z}(0) = 0$. Since $\dot{z}(0) = 0$ there is a time $t \in (0, \tau)$ so that $\epsilon \sin(t) > |z(t)|$. Suppose that $\ddot{z}(t) < 0$ then $z(t) > \frac{1}{2}(z(t) + \epsilon \sin(t))^3 > 0$ a contradiction. Thus $\ddot{z}(t) > 0$ for $t \in (0, \tau)$.

Suppose that $z(t) \leq .3\epsilon \sin(t)$ for some $t \leq \min\{\tau, \pi/2\}$. Call $\beta = \frac{1}{2}(1 + .3)^3$. Then

$$\begin{aligned} \dot{z}(t) &= \int_0^t \ddot{z}(s)ds \leq \int_0^t \frac{1}{2}(.3\epsilon \sin(t) + \epsilon \sin(t))^3 ds \\ &= \beta\epsilon^3[1 - \cos(t) - \frac{1}{3}(1 - \cos(t)^3)]. \end{aligned}$$

Thus

$$\begin{aligned} z(t) &\leq \beta\epsilon^3 \int_0^t [1 - \cos(s) - \frac{1}{3}(1 - \cos(s)^3)]ds \\ &= \beta\epsilon^3 \left[\frac{2}{3}t - \frac{2}{3}\sin(t) - \frac{1}{9}\sin(t)^3\right] \\ &< \beta\epsilon^3(.27)\frac{2}{\pi}t, \text{ by convexity,} \\ &< \beta\epsilon^3(.27)\sin(t), \text{ again by convexity,} \\ &< .3\epsilon^3 \sin(t). \end{aligned} \tag{3.18}$$

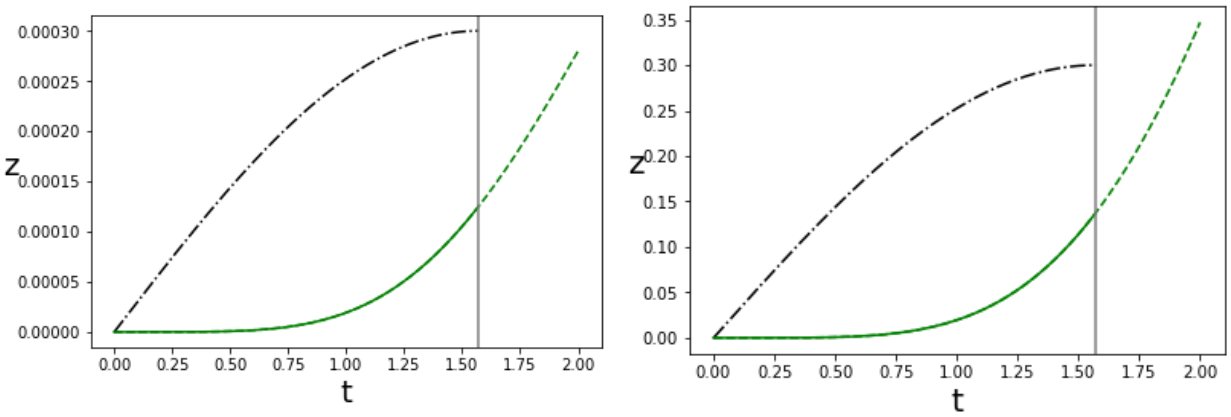

Figure 3.5: Graphs of z in green and $0.3\epsilon^3 \sin(t)$ in black. The vertical gray line is at $\pi/2$. On the left $\epsilon = 0.1$ and on the right $\epsilon = 1$.

Which implies that $z(t) \leq .3\epsilon \sin(t)$ for all $t \leq \min\{\tau, \pi/2\}$. To show that $\tau > \frac{\pi}{2}$ notice that

$$\begin{aligned}(9 + 2\beta)\sin(t)^3 + 12\beta \sin(t) &\geq (9+2)\frac{2}{\pi}t + 12\frac{2}{\pi}t \\ &> 12(1.1)t > 12\beta t,\end{aligned}$$

which implies that $9\sin(t)^3 > 12\beta t - 2\beta \sin(t)^3 - 12\beta \sin(t)$, and multiplying both sides by $\frac{\epsilon^3}{18}$ gives that

$$\frac{1}{2}\epsilon^3 \sin(t)^3 > \beta\epsilon^3 \left[\frac{2}{3}t - \frac{2}{3}\sin(t) - \frac{1}{9}\sin(t)^3\right] \geq z(t)$$

for $t \leq \min\{\tau, \pi/2\}$ by (3.18). On the other hand by the definition of τ

$$z(\tau) = \frac{1}{2}(z(\tau) + \epsilon \sin(t))^3 > \frac{1}{2}\epsilon^3 \sin(\tau)^3.$$

Thus $\tau > \frac{\pi}{2}$.

Therefore $0 \leq z(t) < .3\epsilon^3 \sin(t)$ on $t \in [0, \pi/2]$; see Fig. 3.5. □

Corollary 3.3.17. *Suppose y solves* (3.9) *for a particular $\epsilon \in (0, 1)$, then*

$$\epsilon \sin(t) \leq y(t) \leq \epsilon \sin(t) + .3\epsilon^3 \sin(t), \forall t \in [0, \pi/2]. \tag{3.19}$$

Proof. Apply Lemma 3.3.16 to the fact that $y(t) = z(t) + \epsilon \sin(t)$. □

The bounds for y are used to find bounds for x which solve (3.8) in terms of $x(0) \in (0, 1)$.

Corollary 3.3.18. *Suppose* (x, y) *solves* (3.8) *with* $x(0) = \epsilon \in (0, 1)$*, then for any* $t \in \left[0, \frac{\pi}{2}\right]$,

$$\epsilon \cos(t) - .3\epsilon^3(1 - \cos(t)) \leq x(t) \leq \epsilon \cos(t) + (\epsilon^2 - .3\epsilon^3 + .3\epsilon^4)(1 - \cos(t)) + \frac{1}{2}.3\epsilon^3 t^2. \quad (3.20)$$

Proof. Let $x(0) = \epsilon \in (0, 1)$. Begin with the lower bound. Notice that $y(t) > 0$ on $t \in (0, \frac{\pi}{2}]$, hence $\dot{x} = (x - 1)y > -y$. By the bound for y given in (3.19) gives that

$$x(t) \geq (\epsilon + .3\epsilon^3) \cos(t) - .3\epsilon^3.$$

To find an upper bound consider the second derivative of x for $t \in \left[0, \frac{\pi}{2}\right]$

$$\begin{aligned}
\ddot{x} &= -x + x^2 - \frac{1}{2}y^2 + \frac{1}{2}xy^2 \\
&= (x - 1)\left(x + \frac{1}{2}y^2\right) \\
&\leq (x - 1)x \\
&\leq (\epsilon - 1)\, x.
\end{aligned}$$

Integrating twice reveals an upper bound. The bound of the first derivative is

$$\begin{aligned}
\dot{x}(t) &= \int_0^t \ddot{x}(s)ds \\
&\leq \int_0^t (\epsilon - 1)x(s)ds \\
&\leq \int_0^t (\epsilon - 1)((\epsilon + .3\epsilon^3) \cos(s) - .3\epsilon^3)ds \\
&= (\epsilon - 1)\left(\left(\epsilon + .3\epsilon^3\right) \sin(t) - .3\epsilon^3 t\right) \\
&\leq (\epsilon - 1)\left(\epsilon + .3\epsilon^3\right) \sin(t) + .3\epsilon^3 t
\end{aligned}$$

and hence the bound for x is

$$\begin{aligned} x(t) &= \int_0^t \dot{x}(s)ds \\ &\leq \int_0^t (\epsilon - 1)(\epsilon + .3\epsilon^3)\sin(s) + .3\epsilon^3 s ds \\ &= (1-\epsilon)\left(\epsilon + .3\epsilon^3\right)(\cos(t) - 1) + .15\epsilon^3 t^2 \\ &= \epsilon\cos(t) + \left(\epsilon^2 - .3\epsilon^3 + .3\epsilon^4\right)(1 - \cos(t)) + 0.15\epsilon^3 t^2. \end{aligned}$$

Thus for any $t \in \left[0, \frac{\pi}{2}\right]$,

$$\epsilon\cos(t) - .3\epsilon^3(1-\cos(t)) \leq x(t) \leq \epsilon\cos(t) + \left(\epsilon^2 - .3\epsilon^3 + .3\epsilon^4\right)(1-\cos(t)) + \frac{1}{2}.3\epsilon^3 t^2.$$

□

3.3.3 Range of τ_X and τ_Y

This section is dedicated to finding the ranges of τ_X, τ_Y. First the range of τ_Y is computed, using the bounds of y found in Corollary 3.3.17.

Theorem 3.3.19. *The following hold*

$$\lim_{\epsilon\to 0^+} \tau_Y(\epsilon) = \pi \textit{ and } \lim_{\epsilon\to 1^-} \tau_Y(\epsilon) = \infty.$$

Proof. Let $\{y_\epsilon\}$ be the family of solutions to (3.9) with IC $\epsilon \in [0,1]$. By Lemma 3.3.7 y_1 is monotonically increasing. By Corollary 3.3.13 τ_Y increases in ϵ. Suppose that $\lim_{\epsilon\to 1^-} \tau_Y(\epsilon) = t^* < \infty$, and proceed by contradiction. By Lemma 3.3.14, τ_Y is continuous and by the Lipschitz condition of the ODE,

$$y_1(t^*) = \lim_{\epsilon\to 1^-} y_\epsilon(t^*) = \lim_{\epsilon\to 1^-} y_\epsilon(\tau_Y(\epsilon)) = 0.$$

But $y_1(t^*) \neq 0$, a contradiction, hence

$$\lim_{\epsilon \to 1^-} \tau_Y(\epsilon) = \infty.$$

For the first limit, fix $\epsilon \in (0,1)$. Let y be the solution to (3.9). Let $\theta(t) = \arctan(\frac{\dot{y}}{y})$. Notice

$$\frac{y\left(\frac{\tau_Y(\epsilon)}{2}\right) - y\left(\frac{\pi}{2}\right)}{0 - \dot{y}\left(\frac{\pi}{2}\right)} \geq \left.\frac{1}{d\dot{y}/dy}\right|_{t=\frac{\pi}{2}}, \text{ by (3.15).}$$

So by Corollary 3.3.17, $\epsilon \leq y\left(\frac{\pi}{2}\right) \leq \epsilon + .3\epsilon^3$ for $t = \pi/2$

$$\begin{aligned}
y\left(\frac{\tau_Y(\epsilon)}{2}\right) &\leq y\left(\frac{\pi}{2}\right) - \dot{y}\left(\frac{\pi}{2}\right) \left.\frac{1}{d\dot{y}/dy}\right|_{t=\frac{\pi}{2}}, \text{ by (3.15),} \\
&= y\left(\frac{\pi}{2}\right) + \dot{y}\left(\frac{\pi}{2}\right) \frac{\dot{y}\left(\frac{\pi}{2}\right)}{y\left(\frac{\pi}{2}\right) - \frac{1}{2}y\left(\frac{\pi}{2}\right)^3}, \text{ by } \ddot{y}, \\
&\leq y\left(\frac{\pi}{2}\right) + \frac{\dot{y}(0)^2}{y\left(\frac{\pi}{2}\right) - \frac{1}{2}y\left(\frac{\pi}{2}\right)^3}, \text{ since } \dot{y} \text{ decreases,} \\
&\leq \epsilon + .3\epsilon^3 + \frac{\epsilon^2}{\epsilon}, \text{ applying bounds,} \\
&< 2.3\epsilon.
\end{aligned}$$

By (3.16)

$$\begin{aligned}
\theta(t) &= \theta(0) + \int_0^t -1 + \frac{1}{2}\frac{y(s)^4}{\dot{y}(s)^2 + y(s)^2} ds, \text{ for } t \in \left(0, \frac{\pi}{2}\right] \\
&\leq \frac{\pi}{2} - t + \frac{1}{2}\int_0^t y(s)^2 ds \\
&\leq \frac{\pi}{2} - t + \frac{1}{2}\int_0^t y\left(\frac{\tau_Y(\epsilon)}{2}\right)^2 ds \\
&< \frac{\pi}{2} + (6\epsilon^2 - 1)t.
\end{aligned}$$

So if $\epsilon < \sqrt{6}$ and $t = \frac{\pi/2}{1-6\epsilon^2}$ then $\theta(t) < 0$ and hence $\tau_Y(\epsilon) < \frac{\pi}{1-6\epsilon^2}$. Recall Lemma 3.3.11, which showed that $\tau_Y(\epsilon) > \pi$.

Thus

$$\lim_{\epsilon \to 0^+} \tau_Y(\epsilon) = \pi.$$

□

The range of τ_X is computed, using the bounds of x found in Corollary 3.3.18.

Theorem 3.3.20. *The following hold*

$$\lim_{\epsilon \to 0^+} \tau_X(\epsilon) = \frac{\pi}{2} \text{ and } \lim_{\epsilon \to 1^-} \tau_X(\epsilon) = \infty.$$

Proof. Fix $\epsilon \in (0,1)$. Let (x,y) be the solution to (3.8) with IC $x(0) = \epsilon$. By (3.20) $x\left(\frac{\pi}{2}\right) < 2\epsilon^2$ for sufficiently small ϵ. Since $\ddot{x} = (x-1)\left(x + \frac{1}{2}y^2\right) < 0$ for $t \in [0, \tau_Y(\epsilon)]$, x is concave down on this interval. Thus by concavity, secant slopes decay and so

$$\frac{2\epsilon^2 - \epsilon}{\pi/2 - 0} > \frac{x\left(\frac{\pi}{2}\right) - x(0)}{\pi/2 - 0} \geq \frac{x(\tau_X(\epsilon)) - x(0)}{\tau_X(\epsilon) - 0} = \frac{-\epsilon}{\tau_X(\epsilon)},$$

which implies that $\tau_X(\epsilon) < \frac{\pi}{2} + 2\epsilon$.

Since $\dot{y}\left(\frac{\tau_Y(\epsilon)}{2}\right) = 0, y\left(\frac{\tau_Y(\epsilon)}{2}\right) > 0$ and $\dot{y} = x - \frac{1}{2}y|y|$ means that $x\left(\frac{\tau_Y(\epsilon)}{2}\right) > 0$. Thus $\tau_X(\epsilon) > \tau_Y(\epsilon)/2$ because $x\left(\frac{\tau_Y(\epsilon)}{2}\right) > 0 = x(\tau_X(\epsilon))$ and x decreases on $[0, \tau_Y(\epsilon)]$. Thus

$$\lim_{\epsilon \to 1^-} \tau_X(\epsilon) \geq \lim_{\epsilon \to 1^-} \frac{1}{2}\tau_Y(\epsilon) = \infty.$$

Moreover, $\tau_Y(\epsilon)/2 < \tau_X(\epsilon) < \frac{\pi}{2} + 2\epsilon$. Thus

$$\lim_{\epsilon \to 0^+} \tau_X(\epsilon) = \frac{\pi}{2}.$$

□

This completes Theorem 3.3.3.

3.3.4 Number of Solutions for Symmetric 2-State Follow the Crowd MFG Given Time to Play

It will be shown that the number of different solutions (x, y), over variable IC $x(0)$, of (3.8) constrained by $x(T) = 0$, given T, is a function of the zeros of x. Due to the nature of the zeros of x, the number of solutions depends on the time to play and the behavior of the functions τ_X, τ_Y. Because τ_X, τ_Y are bijective and continuous it can be shown that the number of solutions constrained by $x(T) = 0$ is determined by the ranges of τ_X, τ_Y, see Lemma 3.3.21 and Theorem 3.3.1.

Theorem 3.3.1 gives the number of solutions (θ, u) of the follow the crowd MFG system given by (3.5) with $\theta(0) = \frac{1}{2}$, with time to play T. Using the properties of solutions (x, y) to (3.8), and properties of continuous bijective functions $\tau_X : (0, 1) \twoheadrightarrow (\frac{\pi}{2}, \infty)$ and $\tau_Y : (0, 1) \twoheadrightarrow (\pi, \infty)$, the number of solutions constrained to $x(T) = 0$ can be found given time to play T.

To that end, a lemma discussing the nature of the zeros of x is explored first.

Lemma 3.3.21. *Suppose that (x, y) is a solution to* (3.8) *with IC $x(0) = \epsilon \in (0, 1)$. Then $x(t) = 0$ if and only if $t = \tau_X(\epsilon) + k\tau_Y(\epsilon)$ for $k \in \mathbb{N}_0$.*

Proof. Fix $k \in \mathbb{N}_0$. By Lemma 3.3.9 $x(t) = -x(t + \tau_Y(\epsilon))$ for $t \geq 0$. Therefore

$$|x(\tau_X(\epsilon) + k\tau_Y(\epsilon))| = |x(\tau_X(\epsilon))| = 0.$$

Suppose that $t \in (0, \tau_Y(\epsilon))$ then $|x(\tau_X(\epsilon)+k\tau_Y(\epsilon))+t| = |x(\tau_X(\epsilon)+t)|$. Hence it suffices to show that the function $x(\tau_X(\epsilon)+t)$ has no zeros for $t \in (0, \tau_Y(\epsilon))$. The function $x(\tau_X(\epsilon)+t)$ has no zeros for $t \in (0, \tau_Y(\epsilon))$ because $x(\tau_X(\epsilon)) = x(\tau_X(\epsilon) + \tau_Y(\epsilon)) = 0$ and by Lemma 3.3.9, x is strictly decreasing on $(0, \tau_Y(\epsilon))$ and strictly increasing on $(\tau_Y(\epsilon), 2\tau_Y(\epsilon))$. Hence the conclusion. □

The proof of Theorem 3.3.1 follows from Theorem 3.3.3, or rather the individual conclusions leading up to Theorem 3.3.3.

Proof of Theorem 3.3.1. It suffices to count the solutions (x, y) of (3.8), over all initial conditions $x(0) = \epsilon \in [0, 1]$ such that $x(T) = 0$, given $T > 0$.

Fix $k \in \mathbb{N}$ and $T \in \left(\frac{\pi}{2} + (k-1)\pi, \frac{\pi}{2} + k\pi\right]$. By Theorems 3.3.19 and 3.3.20, for any $n \in \mathbb{N}_0$, $\lim_{\epsilon \to 0^+} \tau_X(\epsilon) + n\tau_Y(\epsilon) = \frac{\pi}{2} + n\pi$. If $\epsilon \in (0, 1)$ is given then by Lemma 3.3.21, $x(T) = 0$ if and only if there exists n such that $\tau_X(\epsilon) + n\tau_Y(\epsilon) = T$.

Suppose $n \geq k$. Then $\lim_{\epsilon \to 0^+} \tau_X(\epsilon) + n\tau_Y(\epsilon) = \frac{\pi}{2} + n\pi \geq \frac{\pi}{2} + k\pi > T$. Since τ_X, τ_Y are strictly monotonically increasing functions, $\tau_X(\epsilon) + n\tau_Y(\epsilon) > T$ for $\epsilon \in (0, 1)$. Instead, suppose n was a negative integer. Then $\tau_X(\epsilon) + n\tau_Y(\epsilon) < 0 < T$ for all $\epsilon \in (0, 1)$ because $\tau_X < \tau_Y$. Thus if $n < 0$ or $n \geq k$ then $x(T) \neq 0$ for any $\epsilon \in (0, 1)$.

Suppose that n is an integer so that $0 \leq n < k$. Then

$$\lim_{\epsilon \to 0^+} \tau_X(\epsilon) + n\tau_Y(\epsilon) = \frac{\pi}{2} + n\pi \leq \frac{\pi}{2} + (k-1)\pi < T < \lim_{\epsilon \to 1^-} \tau_X(\epsilon) + n\tau_Y(\epsilon) = \infty.$$

By Lemma 3.3.14, $\tau_X + n\tau_Y$ is continuous, so an ϵ_n exists such that $\tau_X(\epsilon_n) + n\tau_Y(\epsilon_n) = T$. By Corollary 3.3.13, $\tau_X + n\tau_Y$ is monotonic, so the value ϵ_n where $\tau_X(\epsilon_n) + n\tau_Y(\epsilon_n) = T$ is unique.

By symmetry $x(0) = -\epsilon_n$ for $0 \leq n < k$ give the only solutions so that $x(T) = 0$ and $x(0) < 0$. Finally, for any $T > 0$, $x, y \equiv 0$ is a solution of the IVP, this gives one solution, so $x(0) = 0$ gives that $x(T) = 0$.

Thus there are a total of $1 + 2k$ solutions. □

The solutions of the ITVP initiate as functions identically equal to $1/2$, and increase in magnitude as T increases. Figure 3.6 illustrates all 4 solutions (x, y) such that $y(0) > 0$ with time to play $T = \pi(3 + \frac{1}{2}) + 0.1$. The x and y are plotted together for comparison. Figure 3.7 indicates which MFG solutions are probably fluid limit trajectories by comparing a realization. Figure 3.8 illustrates the increasing number of solutions described in Section 3.3, and Fig. 3.6 demonstrates the solutions plotted with their controls.

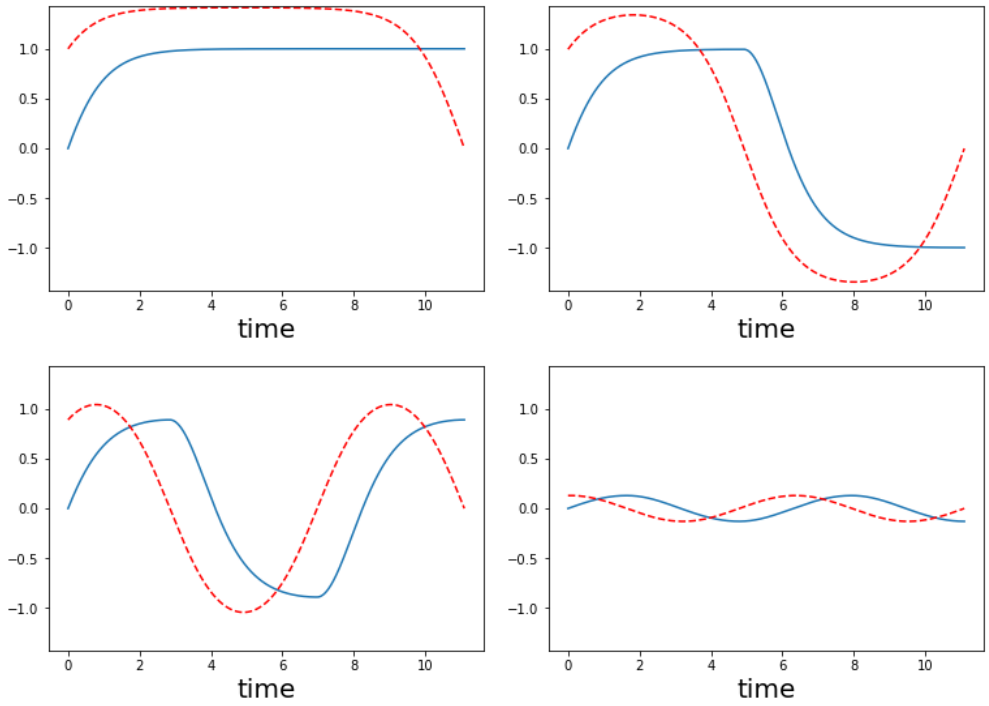

Figure 3.6: Consider (3.6) with $T = \pi(3 + \frac{1}{2}) + 0.1$ and $x(0) = 0$ where $x = 2\theta - 1$. For this amount of running time there are exactly 4 solutions to equation where $y(0) > 0$. The solutions x are plotted (in blue) along with the value $y := u_1 - u_0$ (in red).

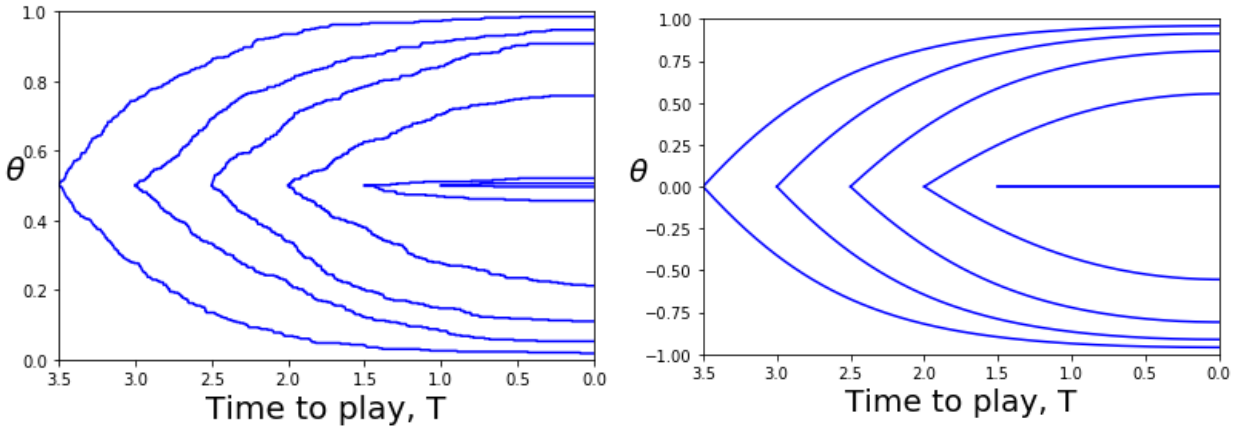

Figure 3.7: On the left, is a set of realizations of the $N + 1$-player game given by (4.3) with 400 players and various time to play. On the right, are the MFG solutions believed to be the fluid limit trajectories. By the symmetries the bifurcation set is identically $1/2$.

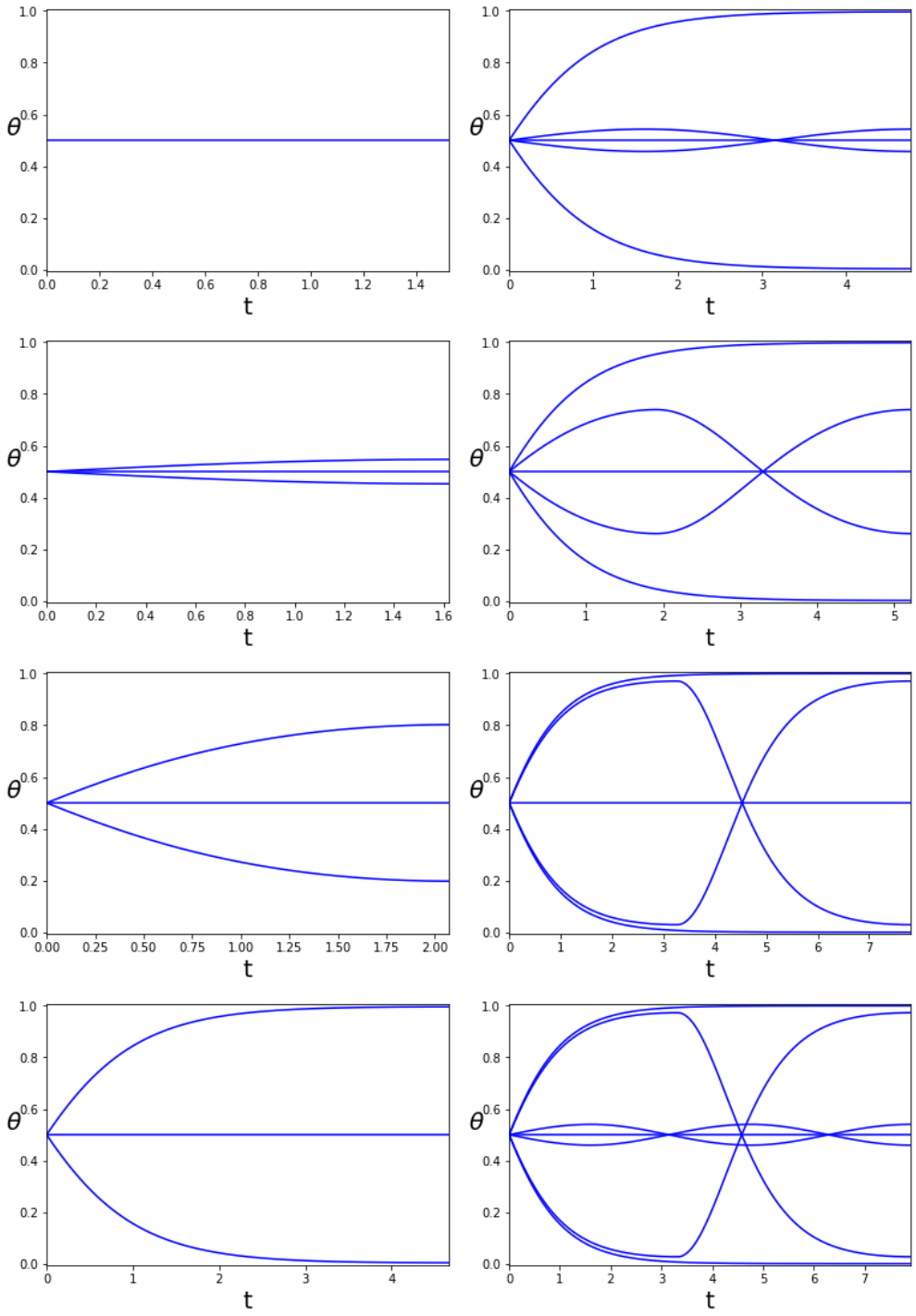

Figure 3.8: Given are all the solutions to (3.6) with $\theta(0) = 1/2$, given various times to play T, in consideration of Theorem 3.3.1. Notice the times before and after an increase of the number of solutions occur.

4 THE MFG MAP AND STABILITY ILLUSTRATIONS

In this chapter, various cost functions will be given in order to illustrate different types of behavior attained by the 2-state MFG model. Stability of the MFG map for the symmetric follow the crowd model from Section 3.3 is analyzed, showing some consistency with Conjecture 2.3.2. The rest of this chapter after that is dedicated to numerical stability, including examples of a *phenomenon* of false positives which are difficult to rectify. Also see Section 2.3.1 for a version of the MFG map which takes smaller iterations to try to improve convergence, especially when given situations where the MFG map maps between multiple functions; see Figs. 2.2 and 2.3.

The assumption of 2-states and of the form of the running cost from Section 2.1.1 are made. Recall the various systems and equations of transition rates.

$$\begin{cases} -\dfrac{d}{dt}u_i = f(i,\theta) - \dfrac{1}{2}(u_i - u_{1-i})_+^2 \\ u_i(T) = \psi_i(\theta(T)), \end{cases} \tag{4.1}$$

with Markov transition probabilities

$$\mathbb{P}[\mathbf{i}_{t+h} = 1 - i | \mathbf{i}_t = i] = (u_i(t) - u_{1-i}(t))_+ h + o(h). \tag{4.2}$$

The cost-to-go functions for the system with $N+1$ rational players are determined by

$$\begin{cases} -\dfrac{d}{dt}u_i^n = f\left(i, \dfrac{n}{N}\right) - \dfrac{1}{2}(u_i^n - u_{1-i}^n)_+^2 + \\ \qquad\qquad + n\alpha_{0,1}^*\left(\dfrac{n-i}{N}, u\right)[u_i^{n+1} - u_i^n] + (N-n)\alpha_{1,0}^*\left(\dfrac{n+1-i}{N}, u\right)[u_i^{n-1} - u_i^n] \\ u_i^n(T) = \psi_i\left(\dfrac{n}{N}\right), \end{cases} \tag{4.3}$$

and the transition rates of the $N+1$ players are given by

$$\begin{aligned}
\mathbb{P}[\mathbf{i}_{t+h} = 1-i | \mathbf{n}_t = n, \mathbf{i}_t = i] &= \alpha^*_{i,1-i}\left(\frac{n}{N}, u^n\right) h + o(h), \\
\mathbb{P}[\mathbf{n}_{t+h} = n-1 | \mathbf{n}_t = n, \mathbf{i}_t = i] &= n\alpha^*_{0,1}\left(\frac{n-i}{N}, u^{n-i}\right) h + o(h) \text{ and} \\
\mathbb{P}[\mathbf{n}_{t+h} = n+1 | \mathbf{n}_t = n, \mathbf{i}_t = i] &= (N-n)\alpha^*_{1,0}\left(\frac{n+1-i}{N}, u^{n+1-i}\right) h + o(h).
\end{aligned} \tag{4.4}$$

Last, the MFG model is

$$\begin{cases}
-\dot{u}_0 = f(0,\theta) - \dfrac{1}{2}(u_0 - u_1)^2_+ \\
-\dot{u}_1 = f(1,\theta) - \dfrac{1}{2}(u_1 - u_0)^2_+ \\
\dot{\theta} = -\theta(u_0 - u_1)_+ + (1-\theta)(u_1 - u_0)_+ \\
u_i(T) = \psi_i(\theta(T)), \theta(0) = \bar{\theta} \in [0,1].
\end{cases} \tag{4.5}$$

The rest of this chapter focuses on stability and numerical results.

4.1 Stability of MFG Map for Follow the Crowd Case

Recall the MFG map from Section 2.3, Φ. The MFG map for the case of the follow the crowd running cost, from Section 3.3, is analyzed. The Gâteaux derivative of the MFG map is evaluated at the MFG solutions, in order to explore the stability of the solutions.

Consider, from Chapter 3, the follow the crowd MFG model given by (3.5) with some time to play T. The MFG map can be expressed in terms of the simplified systems. Consider a continuous function $x : [0,T] \to [-1,1]$ which is considered a prediction to the fluid limit trajectory and let y be the solution to

$$\begin{cases}
-\dot{y} = x - \dfrac{1}{2} y|y| \\
y(T) = 0,
\end{cases} \tag{4.6}$$

and given this y let $\tilde{x}$ be the solution to

$$\begin{cases} \dot{\tilde{x}} = y - \tilde{x}|y| \\ \tilde{x}(0) = x(0). \end{cases} \tag{4.7}$$

Define Φ_X to be the map which takes x to $\tilde{x}$. Then $\Phi_X(2\theta - 1) = 2\Phi(\theta) - 1$, for any prediction θ.

The Gâteaux derivative for Φ_X will be analyzed instead of for Φ. Suppose (x, y) is a solution to (3.6). Fix $\hat{t} \in (0, T)$ and $\epsilon > 0$ sufficiently small. Suppose $h(t) = \delta(t - \hat{t})$. Let $x_\epsilon := x + \epsilon h$. Let y, y_ϵ be the solution to (4.6) with the $x, x_\epsilon : [0, T] \to [-1, 1]$ respectively. Let $k_\epsilon = \frac{1}{\epsilon}(y_\epsilon - y)$. Then

$$\begin{aligned}
\epsilon \dot{k}_\epsilon &= \dot{y}_\epsilon - \dot{y} \\
&= -x_\epsilon + \frac{1}{2} y_\epsilon |y_\epsilon| + x - \frac{1}{2} y|y| \\
&= -\epsilon h + \frac{1}{2}(y + \epsilon k_\epsilon)|y + \epsilon k_\epsilon| - \frac{1}{2} y|y| \\
&= -\epsilon h + \frac{1}{2}(y + \epsilon k_\epsilon)(|y| + \operatorname{sgn}(y)\epsilon k_\epsilon) - \frac{1}{2} y|y| + o(\epsilon^2), \text{ since } y_\epsilon - y = o(\epsilon) \\
&= -\epsilon h + \epsilon k_\epsilon |y| + o(\epsilon^2) \text{ so} \\
\dot{k}_\epsilon &= -h + k_\epsilon |y| + o(\epsilon), \text{ with } k_\epsilon(T) = 0.
\end{aligned}$$

Hence $k_\epsilon(t) = e^{\int_T^t |y| dr} \int_T^t (-h(s) + o(\epsilon)) e^{-\int_T^s |y| dr} ds = e^{-\int_t^{\hat{t}} |y| ds} \mathbb{1}_{\{\hat{t} > t\}} + o(\epsilon)$. Let $\tilde{x}_\epsilon$ be the solution to (4.7) with y_ϵ in place of y, that is $\tilde{x}_\epsilon = \Phi_X(x_\epsilon)$. Let $g_\epsilon = \frac{1}{\epsilon}(\Phi_X(x_\epsilon) - \Phi_X(x))$. Define the limit functions

$$k := \lim_{\epsilon \to 0} \frac{1}{\epsilon}(y_\epsilon - y) \quad \text{and} \quad g := \lim_{\epsilon \to 0} \frac{1}{\epsilon}(\Phi_X(x + \epsilon h) - \Phi_X(x)).$$

Then $k(t) = \mathbb{1}_{\{\hat{t}>t\}} e^{-\int_t^{\hat{t}} |y| ds}$ and

$$\begin{aligned}
\dot{\tilde{x}}_\epsilon - \dot{x} &= y_\epsilon - y - \tilde{x}_\epsilon |y_\epsilon| + x|y| \\
&= \epsilon k_\epsilon - (x + \epsilon g_\epsilon)|y + \epsilon k_\epsilon| + x|y| \\
&= \epsilon k - \epsilon(xk\,\mathrm{sgn}(y) + g_\epsilon |y|) + o(\epsilon^2) \text{ so} \\
\dot{g}_\epsilon &= k(1 - \mathrm{sgn}(y)x) - g_\epsilon |y| + o(\epsilon), \text{ with } g_\epsilon(0) = 0.
\end{aligned}$$

Thus $g(t) = e^{-\int_0^t |y| ds} \int_0^t k(s) e^{\int_0^s |y| dr} (1 - \mathrm{sgn}(y)x) ds$ for the impulse h and given $\hat{t}$. The impulse response is

$$\begin{aligned}
K(t, \hat{t}) &= e^{-\int_0^t |y| dr} \int_0^t \mathbb{1}_{\{\hat{t}>s\}} e^{-\int_s^{\hat{t}} |y| dr} e^{\int_0^s |y| dr} (1 - \mathrm{sgn}(y)x) ds \\
&= \int_0^{t \wedge \hat{t}} e^{-\int_0^t |y| dr} e^{-\int_s^{\hat{t}} |y| dr} e^{\int_0^s |y| dr} (1 - \mathrm{sgn}(y)x) ds \\
&= \int_0^{t \wedge \hat{t}} e^{-\int_0^t |y| dr} e^{-\int_0^{\hat{t}} |y| dr} e^{2\int_0^s |y| dr} (1 - \mathrm{sgn}(y)x) ds. \qquad (4.8)
\end{aligned}$$

Therefore for general solutions (x, y), time to play T, and direction $h : [0, T] \to \mathbb{R}$, the Gâteaux derivative of Φ_X is given by the following integral operator:

$$\begin{aligned}
L_{x,y}(t) &= \int_0^T K(t, \hat{t}) h(\hat{t}) d\hat{t} \\
&= \int_0^T h(\hat{t}) \int_0^{t \wedge \hat{t}} e^{-\int_0^t |y| dr} e^{-\int_0^{\hat{t}} |y| dr} e^{2\int_0^s |y| dr} (1 - \mathrm{sgn}(y)x) ds d\hat{t}. \qquad (4.9)
\end{aligned}$$

Suppose that x is a strictly monotonic solution, then $(1 - \mathrm{sgn}(y(t))x(t)) = e^{-\int_0^t |y| ds}$ by (3.7) and Lemma 3.3.7. Thus $K(t, \hat{t}) = \int_0^{t \wedge \hat{t}} e^{-\int_0^t |y| dr} e^{-\int_0^{\hat{t}} |y| dr} e^{\int_0^s |y| dr} ds$ which is symmetric and

$$L_{x,y}(t) = \int_0^T h(\hat{t}) \int_0^{t \wedge \hat{t}} e^{-\int_0^t |y| dr} e^{-\int_0^{\hat{t}} |y| dr} e^{\int_0^s |y| dr} ds d\hat{t}. \qquad (4.10)$$

The form of (4.10) is relatively simple, and its eigenvalues and eigenfunctions can be

explicitly found in the following special case. Suppose that $x, y \equiv 0$ and $T > 0$. Then $K(t,\hat{t}) = \int_0^{t\wedge\hat{t}} 1ds = \min\{t,\hat{t}\}$. So $K(t,\hat{t}) = K(\hat{t},t)$ and K is positive semidefinite because it is the autocorrelation function for Brownian motion.

Fix integer $n \geq 0$. Suppose that $h_n(t) = \sin(\frac{(2n+1)\pi t}{2T})$. Then

$$\begin{aligned}
L_{x,y}(t) &= \int_0^T \min\{t,\hat{t}\} \sin\left(\frac{(2n+1)\pi\hat{t}}{2T}\right) d\hat{t} \\
&= \int_0^t \hat{t} \sin\left(\frac{(2n+1)\pi\hat{t}}{2T}\right) d\hat{t} + \int_t^T t \sin\left(\frac{(2n+1)\pi\hat{t}}{2T}\right) d\hat{t} \\
&= \left[\left(\frac{2T}{(2n+1)\pi}\right)^2 \sin\left(\frac{(2n+1)\pi\hat{t}}{2T}\right) - \frac{2T}{(2n+1)\pi}\hat{t}\cos\left(\frac{(2n+1)\pi\hat{t}}{+}2T\right)\right]_{\hat{t}=0}^{t} + \\
&\quad + \left[-\frac{2T}{(2n+1)\pi}t\cos\left(\frac{(2n+1)\pi\hat{t}}{2T}\right)\right]_{\hat{t}=t}^{T} = \left(\frac{2T}{(2n+1)\pi}\right)^2 \sin\left(\frac{(2n+1)\pi t}{2T}\right).
\end{aligned}$$

Thus by Mercer's theorem $K(t,s) = \sum_{n=0}^{\infty}\left(\frac{2T}{(2n+1)\pi}\right)^2 \sqrt{\frac{2}{T}}h_n(t)\sqrt{\frac{2}{T}}h_n(s)$. The functions $\sqrt{\frac{T}{2}}h_n(t)$, form an orthonormal basis of functions with the corresponding eigenvalues $\lambda_n = \left(\frac{2T}{(2n+1)\pi}\right)^2$. Notice that $\lambda_0 \geq \lambda_i$ for integer $i \geq 0$. If $T > \frac{\pi}{2}$ then $\lambda_0 = \left(\frac{2}{\pi}T\right)^2 > 1$, hence Φ_X is unstable. If $T < \frac{\pi}{2}$ then $\lambda_0 = \left(\frac{2}{\pi}T\right)^2 < 1$, hence Φ_X is stable.

Recall in Section 3.3 it was shown that $\theta \equiv \frac{1}{2}$ is the unique MFG solution until time to play exceeds $T = \frac{\pi}{2}$. In the corresponding $N+1$ game if one state contains more players than the other then every player attempts to move to that state, so the fluid limit trajectory must be monotone; see Fig. 3.7. That is, the stable points for the MFG map are exactly the fluid limit trajectory at least for $T \in (0, 3\pi/2]$. This is good evidence in support of Conjecture 2.3.2.

One may agree based on the previous computations that it is difficult to show if the MFG map is stable at a given MFG solution. But at least Conjecture 2.3.2 is consistent with the analysis for the case of $x \equiv 0$.

4.2 Stability and Fluid Limit Trajectory

This section is devoted to numerical results for the MFG map Φ for the MFG given by (4.5), with no terminal cost and $f(i,\theta) = |\theta - (1-i)|$. That is the system from Section 3.3 where $y = u_1 - u_0$,

$$\begin{cases} -\dot{y} = 2\theta - 1 - \dfrac{1}{2}y|y|, y(T) = 0 \\ \dot{\theta} = (1-\theta)y_+ - \theta(-y)_+, \theta(0) = \bar{\theta} \in [0,1]. \end{cases} \tag{4.11}$$

To illustrate Conjecture 2.3.2, the MFG map Φ of (4.11) will be put to the test. Consider the time to play $T = \frac{\pi}{2} + 0.01$, then $\Phi^{1000}[\frac{1}{2} + \frac{1}{1000000}\sin(t)](T) \approx 0.5105$, so clearly Φ^n is not approaching $\frac{1}{2}$. On the other hand, if $T = \frac{\pi}{2} + 0.01$, then $\Phi^{1000}[\frac{1}{2} + \frac{1}{1000000}\sin(t)](T) \approx 0.5$ up to 16 decimal places. This is consistent with Conjecture 2.3.2 and the eigenvalues of the map Φ_X about $x \equiv 0$ found in Section 4.1, because $\lambda_0 = \left(\frac{2T}{\pi}\right)^2$. Recall that for $T = \frac{\pi}{2} + 0.01$, $\lambda_0 > 1$ and hence Φ is unstable about $\frac{1}{2}$; and for $T = \frac{\pi}{2} + 0.01$, $\lambda_0 < 1$ and hence Φ is stable about $\frac{1}{2}$.

Consider a large time to play, say $T = 20$, so that multiple MFG solutions exist. The aforementioned conjecture implies that only the monotone solution may be stable, because as discussed the fluid limit trajectories are monotone. Consider two MFG solutions (θ_1, y_1) and (θ_2, y_2) to (4.11), as shown in Fig. 4.1. Conjecture 2.3.2 indicates that the MFG map Φ is stable about θ_1 and unstable about θ_2. The following norms were computed numerically $\|\theta_2 - \Phi^{1000}(\theta_2 + 0.0001)\|_2 = 5.8 * 10^{-07}$, $\|\theta_2 - \Phi^{2000}(\theta_2 + 0.0001)\|_2 = 2.9 * 10^{-10}$ and $\|\theta_2 - \Phi^{3000}(\theta_2 + 0.0001)\|_2 < 1 * 10^{-16}$; indicating stability. This does not bode well for Conjecture 2.3.2.

Let us consider adding noise between iterations, to test stability of Φ at θ_2 another way. Let W^n be independent Wiener processes for each $n \in \mathbb{N}$, and define the process $M_t^n := W_{0.05t}^n$ so that the variance of $M_t^n - M_s^n$ is $0.05(t-s)$. Then define $\theta_2^{n+1} := \Phi(\theta_2^n + M^n)$, with $\theta_2^1 := \theta_2$. Figure 4.2 is a visual aid showing the extent of stability Φ even in the presence of noise. The plots are of the first 100 iterations showing the before and after affects of the

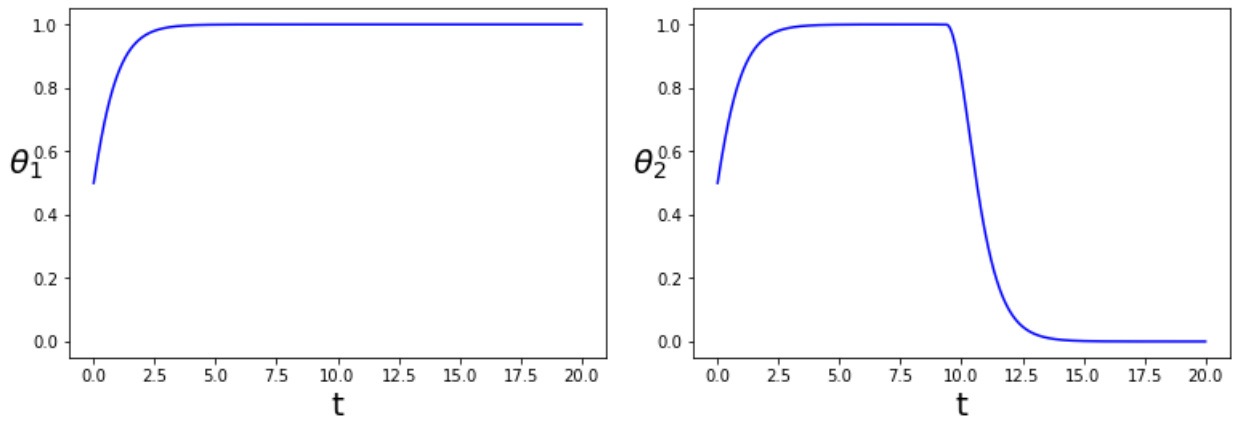

Figure 4.1: The MFG solution on the left is most likely a fluid limit trajectory, and hence by Conjecture 2.3.2 is stable. The MFG solution on the right passes through the value $1/2$, thus by Conjecture 2.3.2 is unstable.

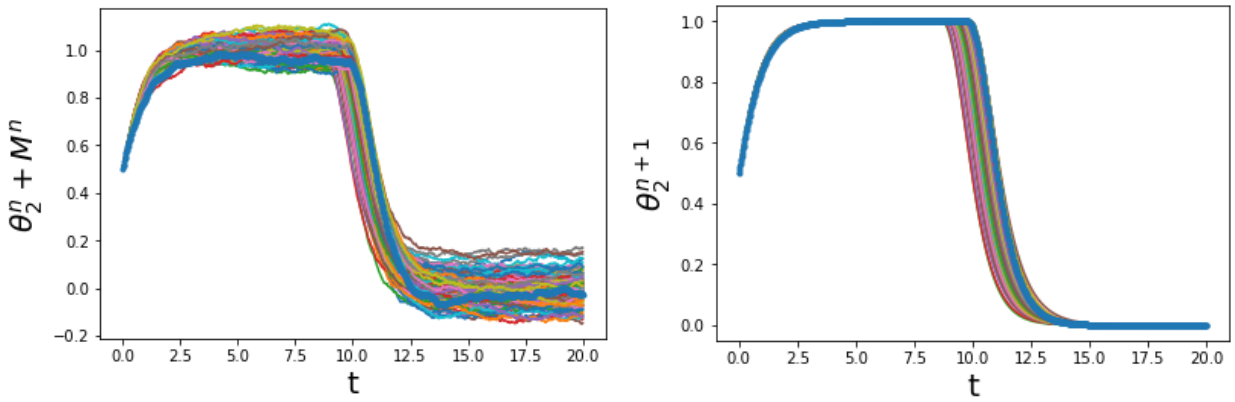

Figure 4.2: On the left are the predictions with noise $\theta_2^n + M^n$. On the right are the plots of θ_2^{n+1} (i.e. $\Phi(\theta_2^n + M^n)$). This is done for $n \in \{1, 2, ..., 100\}$.

map Φ. The functions plotted are $\theta_2^n + M^n$ and θ_2^{n+1}, and the thick line indicates the last iteration, for the purpose of perspective.

Consider the last iteration, θ_2^{101} and let $\theta^* := \Phi^{5000}(\theta_2^{101})$. Numerical computations give that $\|\theta^* - \Phi^{1000}(\theta^*)\|_2 < 1 * 10^{-16}$ indicating stability, and yet $\|\theta_2 - \theta^*\|_2 = 1.734$. The plots of θ_2 and θ^* are given in Fig. 4.3. Since $\theta^* \neq \theta_2$ and crosses the value $1/2$ only once, it cannot be a MFG and hence it cannot be a fixed point, yet it appears to be not only a fixed point but a stable one. This would mean that Φ is stable at a non-fixed point, which is absurd, and thus is nothing more than a numerical anomaly. Thus the local stability

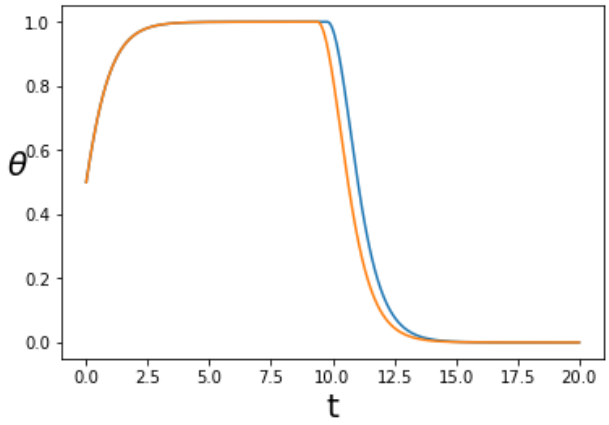

Figure 4.3: In orange is θ_2 and in blue $\theta^* := \Phi^{5000}(\theta_2^{101})$ for given some realization.

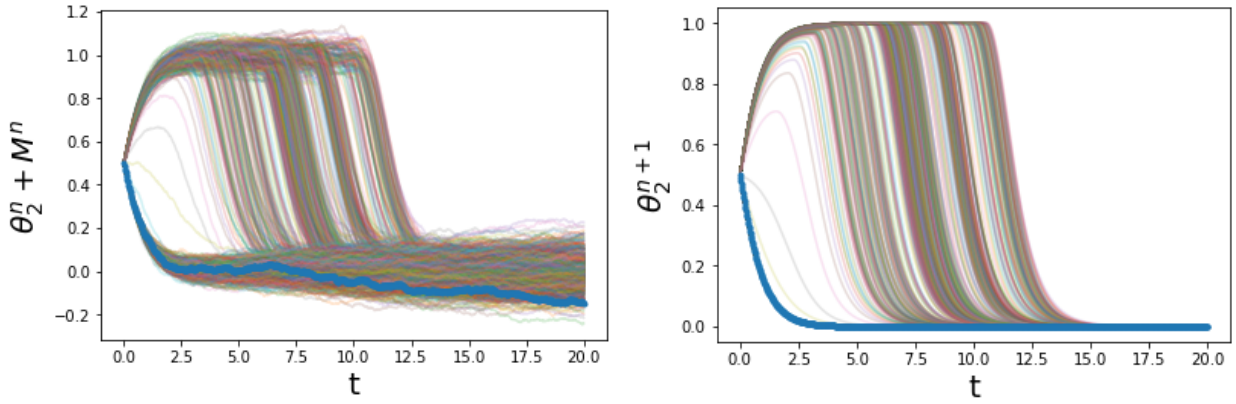

Figure 4.4: On the left are the predictions with noise $\theta_2^n + M^n$. On the right are the plots of θ_2^{n+1} (i.e. $\Phi(\theta_2^n + M^n)$). This is done for $n \in \{1, 2, ..., 1000\}$ and some realization. Opacity is added to illustrate the number of overlaying trajectories.

indicated numerically at θ_2 before may be a result of this same numerical phenomenon, and Conjecture 2.3.2 may indeed hold. For no other reason but to give an intuition, lets evaluate θ_2^n for more values of n; see Fig. 4.4. Figure 4.5 gives two different realizations of θ_2^{301} and then, showing each iteration, finds the limit of $\Phi^n(\theta_2^{301})$ to be $\pm\theta_1$, the other fluid limit trajectories. This figure indicates that the domain of attraction due to the numerical phenomenon is quite small.

To illustrate stability for the monotone increasing solution significantly more noise is added between the iterations of Φ. Recall the independent Wiener processes W^n and define the processes $N_t^n := W_{0.2t}^n$ so that the variance of $N_t^n - N_s^n$ is $0.2(t-s)$. Then define

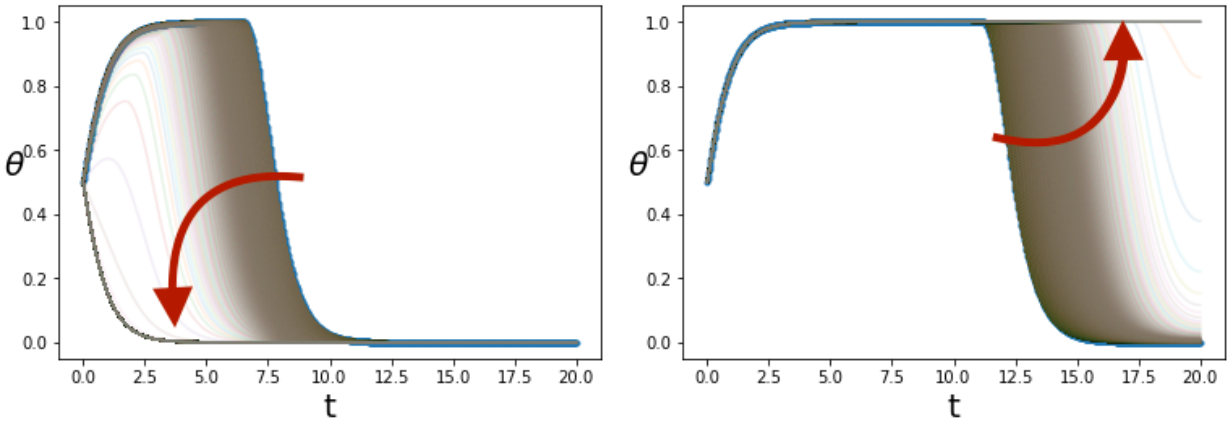

Figure 4.5: The two plots are two different realizations. In thick blue is θ_2^{301}, the rest are $\Phi^n(\theta_2^{301})$, this is done for $n \in \{1, 2, ..., 10000\}$. The plot on the left shows $\Phi^n(\theta_2^{301})$ approaching $-\theta_1$ and the plot on the right shows $\Phi^n(\theta_2^{301})$ approaching θ_1 Opacity is added to illustrate time spent.

$\theta_1^{n+1} := \Phi(\theta_1^n + N^n)$, with $\theta_1^1 := \theta_1$. Figure 4.6 shows $\theta_1^n + N^n$ for $n \in \{1, 2, ..., 200\}$, and it can be seen that even with higher variance the functions θ_1^n are relatively close. Moreover, the value $\|\theta_1 - \Phi^{1000}(\theta_1^{200})\|_2 < 1 * 10^{-16}$ based on numerics, giving a strong indication of stability. Figures 4.4, 4.5 and 4.6, indicate that the fluid limit trajectory may be stable with a wide domain of attraction.

Consider solutions to (4.11) with time to play $T = 50$. For time to play being this large, pseudo-stable fixed points exist which appear to be numerically close to a piece-wise combination of two different MFG solutions. Call the dashed green curve in Fig. 4.7, θ. The function $\Phi^{1000}(\theta)$, which is plotted in dark green on the right, appears to be a fixed point as $\|\Phi^{2000}(\theta) - \Phi^{1000}(\theta)\| < 1 * 10^{-16}$. These examples indicate some of the difficulties which will arise in MFGs when uniqueness is not guaranteed.

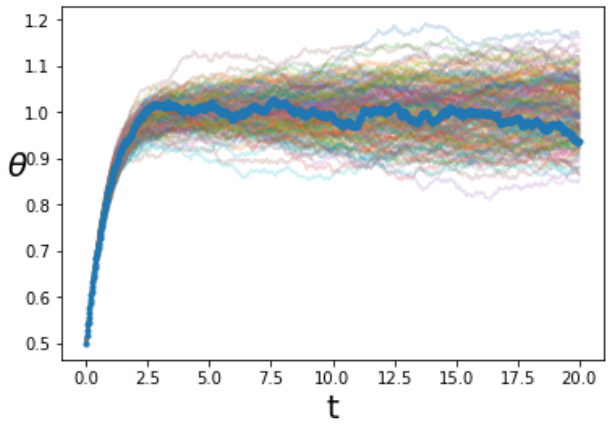

Figure 4.6: In thick blue $\theta_1^{200} + N^{200}$. The rest are $\theta_1^n + N^n$. This is done for $n \in \{1, 2, ..., 199\}$. Opacity is added to illustrate the number of overlaying trajectories.

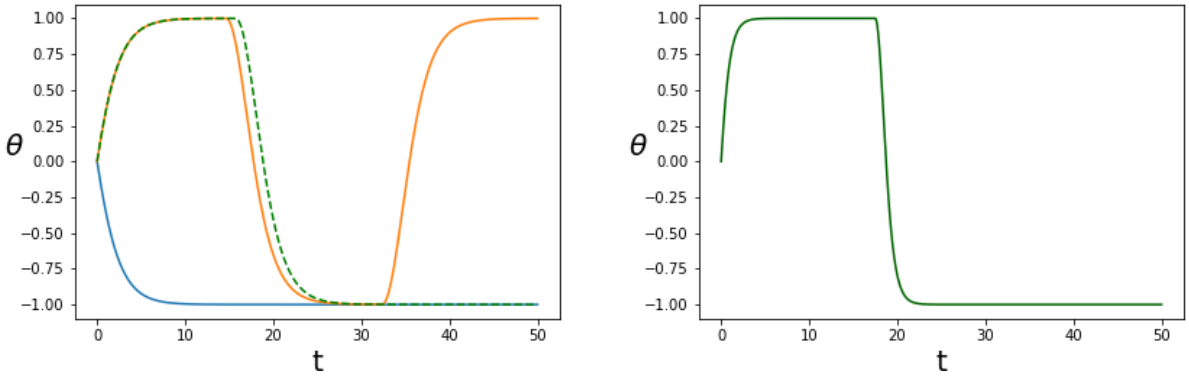

Figure 4.7: The plot to the left has three functions. In blue and orange are two solutions to (4.11). In green, θ, is a curve that starts off following the orange curve somewhat closely and then follows the blue curve. The plot to the left in dark green is $\Phi^{1000}(\theta)$.

4.3 Indifference Sets and Heat Maps

This section gives examples of the 2-state MFG given by (4.5) with various running and terminal costs. With each example are heat maps associated with the cost-to-go function given by the $N+1$ player game described by (4.3). These examples give a visual of the cost-to-go functions, which gives an idea of what the fluid limit trajectories may look like.

Consider (4.3) with time to play $T > 0$. Also consider the map

$$t \mapsto \{n : u_1^n(t) - u_0^n(t) > 0 \text{ and } u_1^{n+1}(t) - u_0^{n+1}(t) < 0\}/(N+1),$$

denoted η_T^N. Recall that there is a dependency for u_0^n and u_1^n on N, which is dropped from the notation. Suppose that $\lim_{N\to\infty} \eta_T^N$ converges to say η_T. Then the indifference set is exactly the set of points $(T-t, \eta_T(t))$ for $0 \le t \le T$ and for any $T > 0$.

Below are figures of many examples, with different running and terminal costs. In the first two examples, the fluid limit trajectories are plotted over the heat map of $u_1^n(t) - u_0^n(t)$ starting at the indifference curve to illustrate how the two relate; see Figs. 4.8 and 4.10. The next example is of a prisoners' dilemma with social pressure running cost, this example is interesting because the indifference curve crosses $1/2$; see Fig. 4.11. Also illustrated is a sequence of indifference curves converging, η_T^N, converges pointwise; see Fig. 4.12.

Figures 4.13 and 4.14 show two examples with follow the crowd running cost but also with the same non-constant terminal cost added to both states. Certainly the MFG solutions are the same as if no terminal costs were added because the difference of the terminal costs over the states is zero. What is interesting about these figures is how the fluid limit trajectories follow the level sets of the heat map of u_0^n fairly well. The last heat maps correspond with the example given in Section 2.3.1. In each figure $N = 400$ except in Fig. 4.12. The red/blue plots below, the line where the red meets the blue from above (red over blue in the red and blue plots) is the indifference curve.

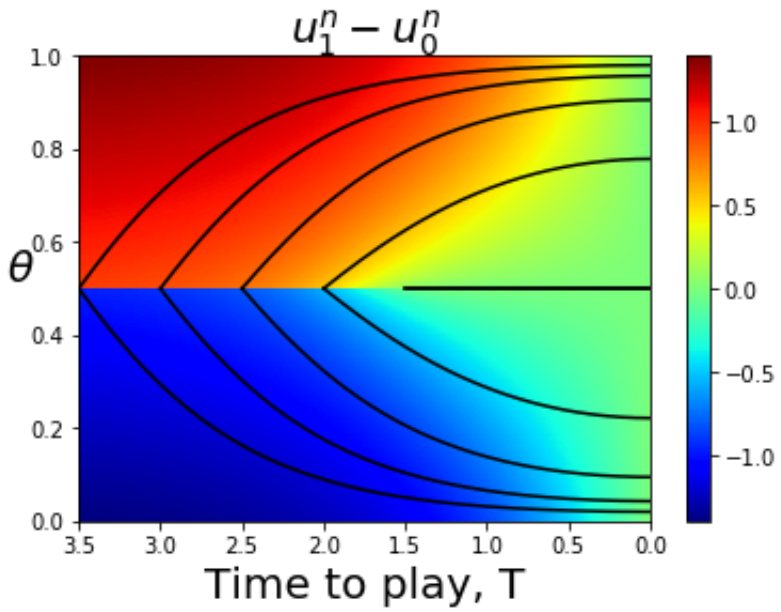

Figure 4.8: The fluid limit trajectories which are MFG solutions overlaid on the cost-to-go difference $u_1^n - u_0^n$. Notice the relationship between the colors from the heat map and the derivative of the curves.

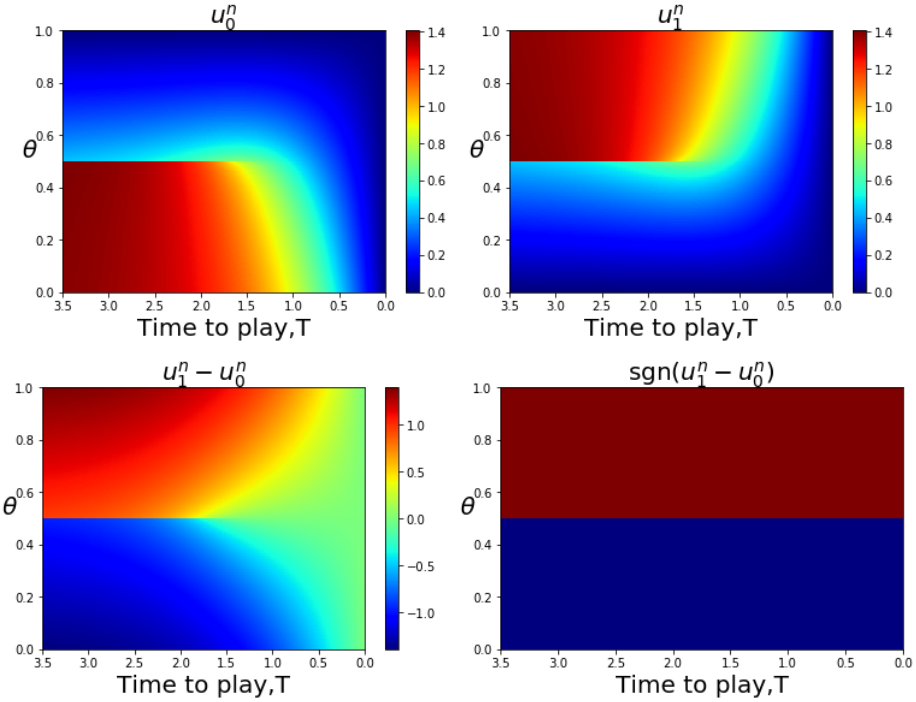

Figure 4.9: Cost-to-go heat maps for follow the crowd example. No terminal costs, and $f(i, \theta) = |\theta - (1 - i)|$. Cost-to-go values for both states are shown in the top two plots respectively. Bottom left is the difference, and bottom right is the sign of the difference.

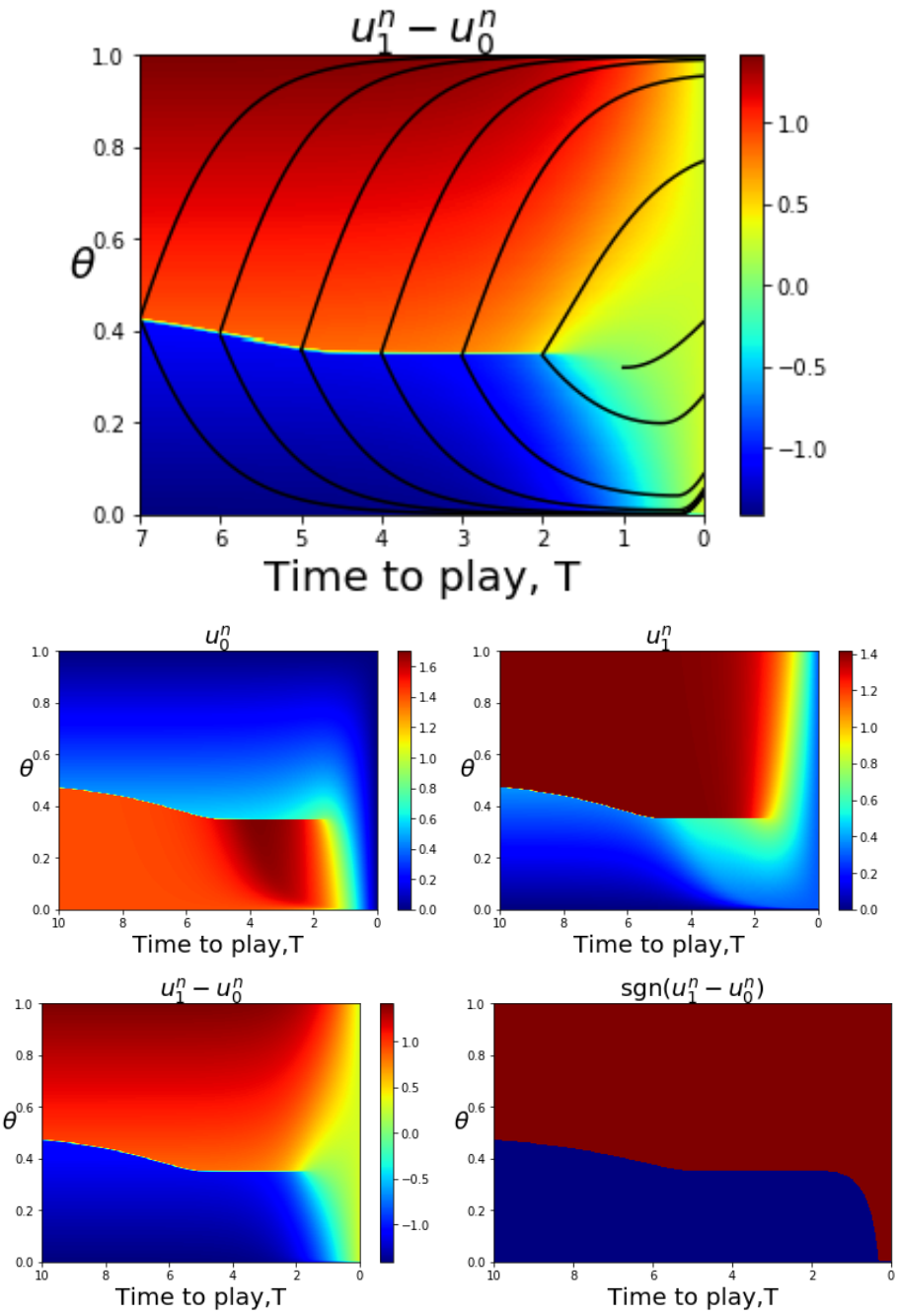

Figure 4.10: Cost-to-go heat maps for follow the crowd example with terminal cost on one state. Terminal cost of 0.3 for all players in state 1 and no terminal cost for players in state 0. Running cost has $f(i, \theta) = |\theta - (1 - i)|$. Note how only the existence of a terminal cost explains why the curve of the graph in $\mathrm{sgn}(u_1^n - u_0^n)$ drops so quickly, for small time to go.

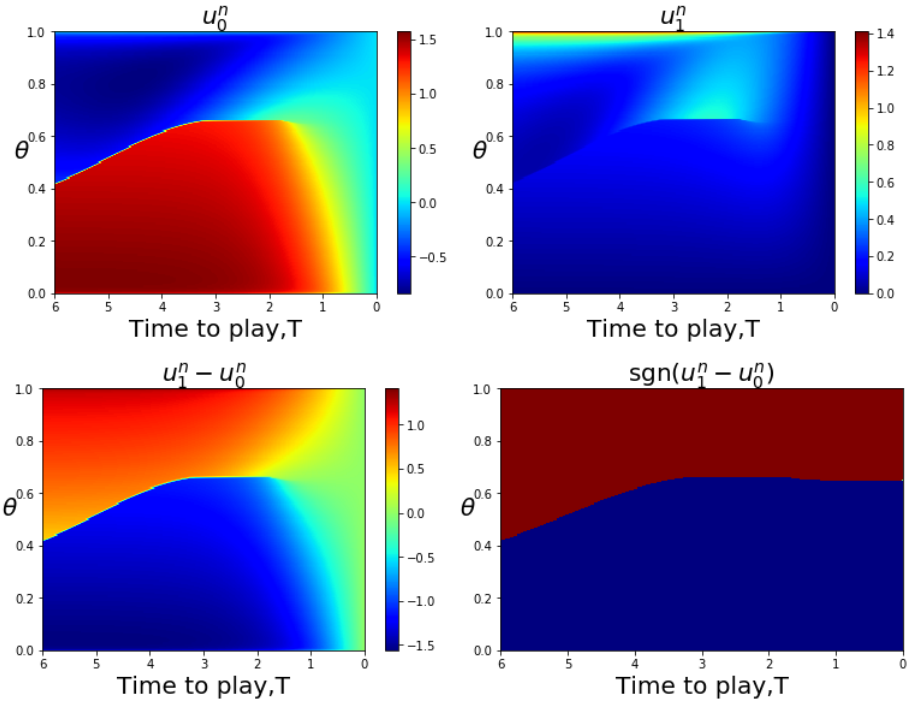

Figure 4.11: Cost-to-go heat maps for an example with follow the crowd tendency with a prisoners' dilemma cost added in. The prisoners' dilemma associated cost is such that state 0 is the cooperative state and state 1 is the greedy state. No terminal cost exists. The social pressure cost is given by $|1 - i - \theta|$, the cooperative cost is given by 0.6θ, and the individual incentive cost is given by $0.3\mathbb{1}_{i=0}$. Running cost has $f(i, \theta) = |1 - i - \theta| - 0.6\theta + 0.3\mathbb{1}_{i=0}$.

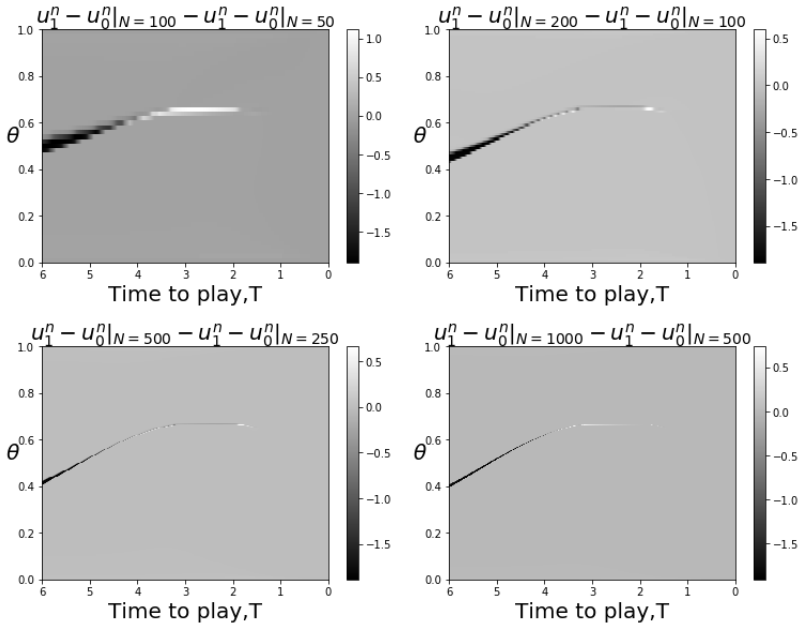

Figure 4.12: Illustration of the pointwise convergence of the indifference set shown in Fig. 4.11.

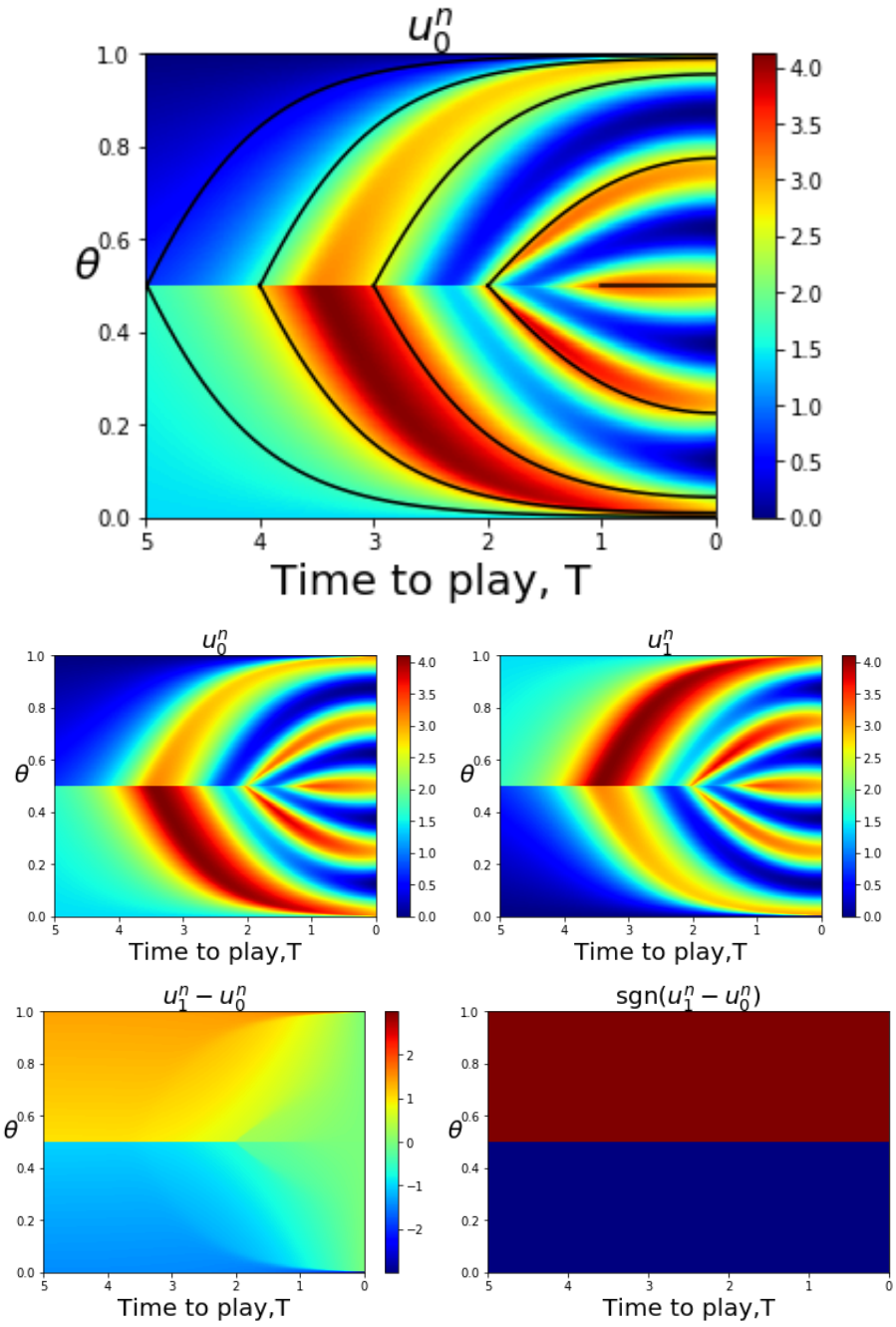

Figure 4.13: Cost-to-go heat maps for follow the crowd example with terminal cost for each state given by $3\cos(4\pi\frac{n}{N})^2$. Running cost has $f(i,\theta) = |\theta - (1-i)|$.

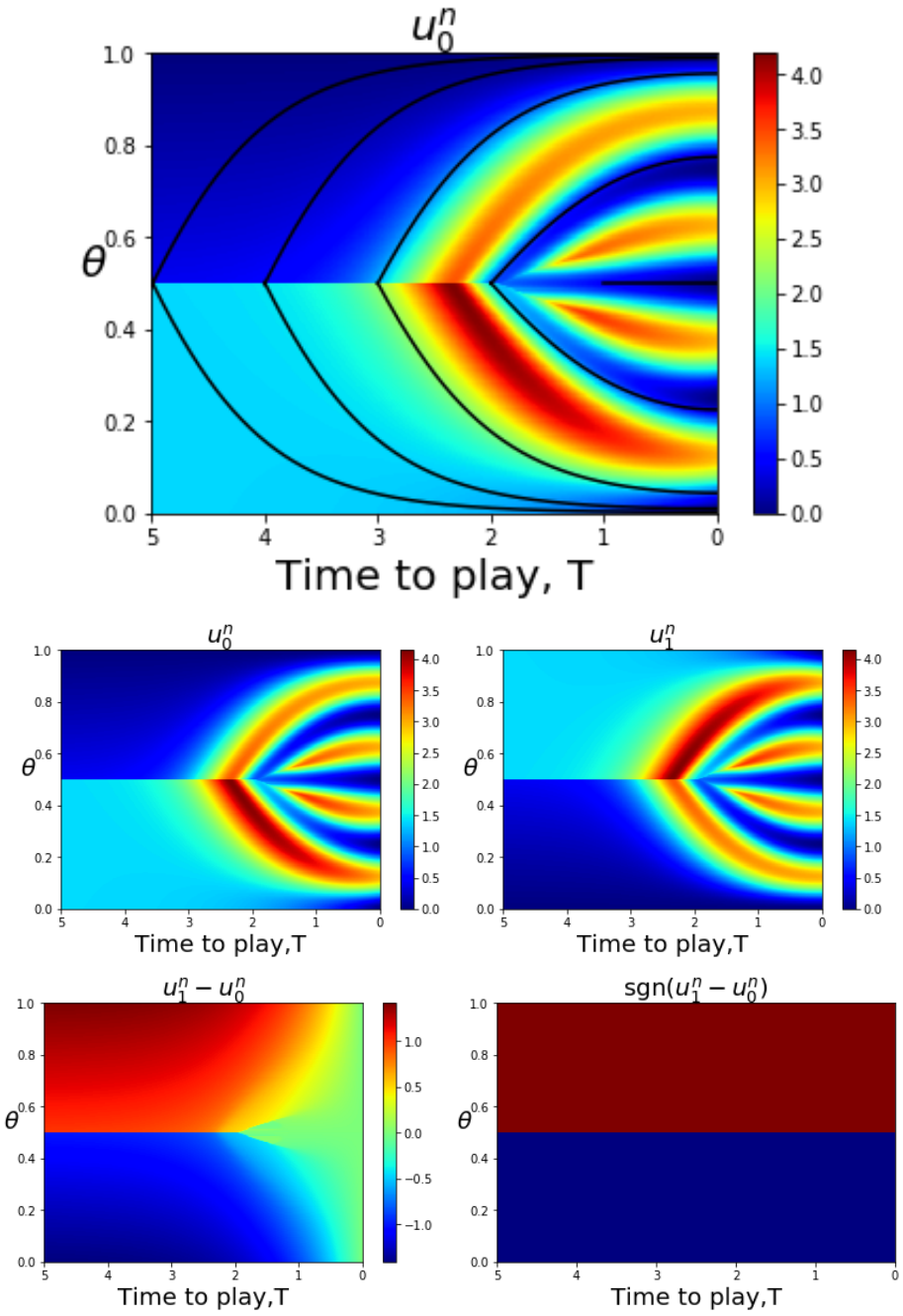

Figure 4.14: Cost-to-go heat maps for follow the crowd example with terminal cost for each state given by $3\sin(4\pi\frac{n}{N})^2$. Running cost has $f(i,\theta) = |\theta - (1-i)|$.

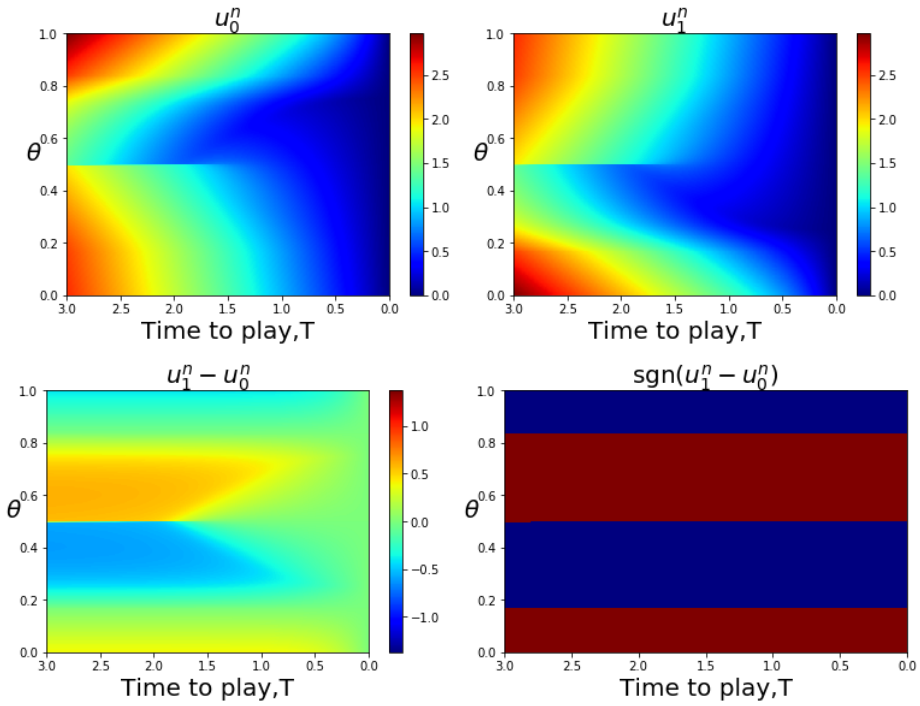

Figure 4.15: Cost-to-go heat maps for an example with follow the crowd tendency with a congestion cost for extreme imbalance. No terminal cost exists. Running cost has $f(i,\theta) = |1 - i - \theta| + 8(\theta - 0.75)\mathbb{1}_{\{\theta > 0.75\}} + 8(0.25 - \theta)\mathbb{1}_{\{\theta < 0.25\}}$.

5 CONCLUSION

In Chapter 3 two tractable examples of 2-state MFGs are investigated, one having unique solutions and the other having non-unique solutions. When dealing with non-unique solutions they begin as the fluid limit trajectory for short enough time to play, but as the time to play increases these solutions continued past the bifurcation curve and lose their relevance to the original game.

Analysis of an example in Sections 3.3 and 4.1 was given which showed that Conjecture 2.3.2 holds for $T \in (0, 3\pi/2]$ in this example. The numerical phenomenon investigated in Chapter 4 displays numerical stability for points which are not analytically fixed points. This makes Conjecture 2.3.2 difficult to dismiss based on numerics alone.

In Section 4.2, however, an example is thoroughly explored indicating that even if Conjecture 2.3.2 were true, numerical methods based on it have limited practical value. A better numerical method for finding the fluid limit trajectories may be to discretize the derivative of the MFG map and check its eigenvalues; this was not investigated in this thesis.

REFERENCES

[1] M. Huang, R. P. Malhamé, P. E. Caines et al., "Large population stochastic dynamic games: Closed-loop Mckean-Vlasov systems and the Nash certainty equivalence principle," *Communications in Information & Systems*, vol. 6, no. 3, pp. 221–252, 2006.

[2] J.-M. Lasry and P.-L. Lions, "Mean field games," *Japanese Journal of Mathematics*, vol. 2, no. 1, pp. 229–260, 2007.

[3] P. Cardaliaguet, F. Delarue, J.-M. Lasry, and P.-L. Lions, "The master equation and the convergence problem in mean field games," *arXiv preprint arXiv:1509.02505*, 2015.

[4] P.-L. Lions and J.-M. Lasry, "Large investor trading impacts on volatility," in *Paris-Princeton Lectures on Mathematical Finance 2004*. Springer, 2007, pp. 173–190.

[5] M. Huang, P. E. Caines, and R. P. Malhamé, "Large-population cost-coupled LQG problems with nonuniform agents: Individual-mass behavior and decentralized ε-Nash equilibria," *IEEE Transactions on Automatic Control*, vol. 52, no. 9, pp. 1560–1571, 2007.

[6] Y. Achdou, F. J. Buera, J.-M. Lasry, P.-L. Lions, and B. Moll, "Partial differential equation models in macroeconomics," *Phil. Trans. R. Soc. A*, vol. 372, no. 2028, p. 20130397, 2014.

[7] D. A. Gomes, J. Mohr, and R. R. Souza, "Continuous time finite state mean field games," *Applied Mathematics & Optimization*, vol. 68, no. 1, pp. 99–143, 2013.

[8] R. Carmona and F. Delarue, "The master equation for large population equilibriums," in *Stochastic Analysis and Applications 2014*. Springer, 2014, pp. 77–128.

[9] A. Bensoussan, J. Frehse, and S. C. P. Yam, "The master equation in mean field theory," *Journal de Mathématiques Pures et Appliquées*, vol. 103, no. 6, pp. 1441–1474, 2015.

[10] V. N. Kolokoltsov, M. Troeva, and W. Yang, "On the rate of convergence for the mean-field approximation of controlled diffusions with large number of players," *Dynamic Games and Applications*, vol. 4, no. 2, pp. 208–230, 2014.

[11] H. Yin, P. G. Mehta, S. P. Meyn, and U. V. Shanbhag, "Synchronization of coupled oscillators is a game," *IEEE Transactions on Automatic Control*, vol. 57, no. 4, pp. 920–935, 2012.